

## MiR-191 inhibit angiogenesis after acute ischemic stroke targeting VEZF1

Kang Du<sup>1,2,\*</sup>, Can Zhao<sup>1,2,\*</sup>, Li Wang<sup>1,2</sup>, Yue Wang<sup>1,2</sup>, Kang-Zhen Zhang<sup>1,2</sup>, Xi-Yu Shen<sup>1,2</sup>, Hui-Xian Sun<sup>1,2</sup>, Wei Gao<sup>1,2</sup>, Xiang Lu<sup>1,2</sup>

<sup>1</sup>Department of Geriatrics, Sir Run Run Hospital, Nanjing Medical University, Nanjing, Jiangsu Province 211166, China

<sup>2</sup>Key Laboratory for Aging and Disease, Nanjing Medical University, Nanjing, Jiangsu Province 211166, China

\*Equal contribution

**Correspondence to:** Wei Gao, Xiang Lu; **email:** [gaowei84@njmu.edu.cn](mailto:gaowei84@njmu.edu.cn), [luxiang66@njmu.edu.cn](mailto:luxiang66@njmu.edu.cn)

**Keywords:** acute stroke, angiogenesis factor, miR-191, VEZF1

**Received:** February 15, 2019

**Accepted:** April 29, 2019

**Published:** May 7, 2019

**Copyright:** Du et al. This is an open-access article distributed under the terms of the Creative Commons Attribution License (CC BY 3.0), which permits unrestricted use, distribution, and reproduction in any medium, provided the original author and source are credited.

### ABSTRACT

Acute ischemic stroke (AIS) is a major public health problem in China. Impaired angiogenesis plays crucial roles in the development of ischemic cerebral injury. Recent studies have identified that microRNAs (miRNAs) are important regulators of angiogenesis, but little is known the exact effects of angiogenesis-associated miRNAs in AIS. In the present study, we detected the expression levels of angiogenesis-associated miRNAs in AIS patients, middle cerebral artery occlusion (MCAO) rats, and oxygen-glucose deprivation/reoxygenation (OGD/R) human umbilical vein endothelial cells (HUVECs). MiR-191 was increased in the plasma of AIS patients, OGD/R HUVECs, and the plasma and brain of MCAO rats. Over-expression of miR-191 promoted apoptosis, but reduced the proliferation, migration, tube-forming and spheroid sprouting activity in HUVECs OGD/R model. Mechanically, vascular endothelial zinc finger 1 (VEZF1) was identified as the direct target of miR-191, and could be regulated by miR-191 at post-translational level. In vivo studies applying miR-191 antagomir demonstrated that inhibition of miR-191 reduced infarction volume in MCAO rats. In conclusion, our data reveal a novel role of miR-191 in promoting ischemic brain injury through inhibiting angiogenesis via targeting VEZF1. Therefore, miR-191 may serve as a biomarker or a therapeutic target for AIS.

### INTRODUCTION

Acute ischemic stroke (AIS) is a major cerebrovascular disease ascribing to the sudden reduction of cerebral blood flow, characterized by a series of cellular and molecular disturbances. With a mortality rate of 10.3% and a morbidity rate of 19.7% in China [1], ischemic stroke is the leading cause of death and disability worldwide [2]. Several common risk factors, including hypertension, diabetes, dyslipidemia, alcohol, smoking, and inflammation [3–5], have been identified to be related to the pathogenesis of AIS. It is generally accepted that impaired

neurovascular repair, especially angiogenesis, plays crucial roles in the development of ischemic cerebral injury [6].

Angiogenesis is the physiological process through which new blood vessels form by the extension or elaboration of existing vessels [7]. This process depending on endothelial cells is under the control of an extensive variety of angiogenic stimulators and inhibitors [8]. A growing number of studies have shown that microRNAs (miRNAs) are involved in the regulation of angiogenesis in ischemic diseases, including AIS [9–11].

MiRNAs are ~22nt RNAs that mediate posttranscriptional regulation of mRNA targets by binding to their 3' un-translated region (UTRs) in diverse eukaryotic lineages [12]. Changes of MiRNA expression profile have been detected in AIS patients [13], middle cerebral artery occlusion (MCAO) rats [14] and oxygen-glucose deprivation/reoxygenation (OGD/R) cells [15–17]. Particularly, several angiogenesis-associated miRNAs, such as miR-210 [18, 19], miR-21 [20, 21], miR-126 [22, 23], miR-155 [24, 25], miR-31 [26], miR-223-3p [27], miR-191 [28] and miR-361 [29], are altered in patients with AIS and injured endothelial cells. However, the mechanism underlying the role of angiogenesis-associated miRNAs in AIS remains to be further explored.

Thus, the aim of the present study was to investigate the effects of angiogenesis-associated miRNAs in the angiogenesis after AIS both *in vitro* and *in vivo*.

## RESULTS

### Screening of miRNAs

To exclude tumor-related angiogenesis, we retrieved all published miRNAs related to the angiogenesis of endothelial cell in Pubmed (32 miRNAs, Table 1). After excluded 24 miRNAs that have been shown to play definite roles in acute stroke, we selected 8 miRNAs for further study (Table 2).

### Characteristics of enrollment patients

We enrolled 6 AIS patients and 6 control subjects as Cohort A, and another 12 AIS patients and 12 control subjects as Cohort B. Characteristics of Cohort A and B were shown in Table 3 and Table 4, respectively. There was no statistically difference of demographic or vascular risk factors between AIS patients and controls.

### Expressions of miRNAs in AIS patients

Eight angiogenesis-associated miRNAs (miR-361 [29], miR-29a [30], miR-31 [26], miR-223-3p [27], miR-640 [31], miR-193a-3p [32], miR-191 [28], miR-503 [33]) levels were first measured in Cohort A. The expression of miR-361, miR-31, miR-223-3p, and miR-191 were changed in AIS patients when compared to the controls (Supplementary Figure 1B, 1C, 1E, 1F). These four miRNAs, including miR-31 (Figure 1A), miR-191 (Figure 1B), miR-223-3p (Figure 1C), and miR-361 (Figure 1D) were further detected in Cohort B. However, only miR-191 was higher in AIS patients than those controls (Figure 1B). The chart 1 showed the screening process.

### Expression of miR-191 in rat MCAO model and OGD/R HUVECs

Consistently, miR-191 levels were increased in the plasma of rat MCAO model both at 24h and 48h after reperfusion [14, 34] (Figure 1E, 1F). However, no significant difference of miR-191 levels was observed between the two time points (data not shown). The expression of miR-191 was also increased in the ischemic boundary zone (IBZ) (Figure 1G). We further detected miR-191 in HUVECs and found that miR-191 expression was elevated in OGD/R group (Figure 1H).

### Function of miR-191 in HUVECs proliferation

We transfected HUVECs with 50nM miR-191 mimic and 100nM miR-191 inhibitor to up and down-regulate the expression of miR-191, respectively (Figure 2A, 2B). HUVECs were then subjected to reoxygenation for 18h after 2h of OGD. We found that up-regulation of miR-191 significantly reduced HUVEC proliferation (Figure 2C), while down-regulation of miR-191 promoted the proliferation (Figure 2D).

### Function of miR-191 in HUVECs apoptosis and cell cycle

By using flow cytometry, we showed that up-regulation of miR-191 increased the apoptosis rate of HUVECs (Figure 3A, 3C), while down-regulation of miR-191 ameliorated the apoptosis induced by OGD/R (Figure 3B, 3D). We also found that over-expression of miR-191 blocked the cell cycle in the S phase (Figure 3E, 3G), which is consistent with the study of Gu, Y., et al. [35]. However, silence of miR-191 only slightly increased the number of G2 cells (Figure 3F, 3H).

### Function of miR-191 in HUVECs migration

To investigate the function of miR-191 in HUVECs migration in OGD/R, scratch wound healing assay and transwell migration assay were performed. Over-expression of miR-191 significantly delayed the closure of scratch wounds (Figure 4A, 4C) and markedly reduced the number of migrated cells (Figure 4E, 4G). In contrast, inhibition of miR-191 promoted the healing of scratch wounds (Figure 4B, 4D) and enhanced cell migration (Figure 4F, 4H).

### Function of miR-191 in HUVECs tube-forming activity

We found that transfection of HUVECs with miR-191 mimic reduced the number of newly developed tube meshes when compared with controls (Figure 5A, 5C).

**Table 1. Endothelial angiogenesis associated miRNAs.**

miRNA names	Cell types	miRNA target(s)	Impact on angiogenesis	References(PMID)
miR-210	HUVEC	EFNA3	promote	18417479
miR-424	HUVEC;BOEC;MVEC	CUL2	promote	20972335
miR-200b	HMEC	ETS1	inhibit	21081489
miR-24	HUVEC	GATA2;PAK4	inhibit	21788589
miR-21	HPAEC	RhoB; Rho-kinase	promote	22371328
miR-125b	HUVEC	VE-cadherin	inhibit	22391569
miR-361	HUVEC	VEGF	inhibit	23128854
Let-7;miR-103	HUVEC	AGO1	promote	23426184
miR-29a	HUVEC	HBP1	promote	23541945
miR-93	HUVEC	P21; E2F-1; P53	promote	23559675
miR-320	HUVEC	NRP1	inhibit	24114198
miR-31	EPC	FAT4;TBXA2R	promote	24558106
miR-101	HUVEC	Cul3	promote	24844779
miR-221	EPC	PIK3R1	inhibit	25236949
miR-222	EPC	ETS1	inhibit	25236949
miR-223-3p	CMEC	RPS6KB1;HIF-1 $\alpha$	inhibit	25313822
miR-429	HUVEC	HIF-1 $\alpha$	inhibit	25550463
miR-107	RBMECs; HUVECs	Dicer-1	promote	26294080
miR-185	HMEC-1	STIM1	inhibit	26694763
miR-640	HUVEC	HIF-1 $\alpha$	inhibit	26879375
miR-140-5p	HUVEC	VEGF	inhibit	27035554
miR-126	EPC;ESC	SPRED1; PIK3R2/p85 $\beta$	promote	27180261
miR-195	hEPC	GABARAPL1	inhibit	27623937
miR-155	HUVEC	E2F2	promote	27731397
miR-193a-3p	ECFC	HMGB1	inhibit	28276476
miR-186	HUVEC	HIF-1 $\alpha$	inhibit	28571741
miR-153-3p	HUVEC	HIF-1 $\alpha$	inhibit	28985553
miR-191	HUVEC	HIF-2 $\alpha$	inhibit	30090327
miR-503	EPC	Apelin	promote	29800588
miR-19b	HUVEC	TGF $\beta$ 2	inhibit	30425199
miR-19a	HUVEC	EDNRB	inhibit	30550764

Abbreviations: HUVEC: human umbilical vein endothelial cells; BOEC: blood outgrowth endothelial cells; MVEC: microvasculature endothelial cells; HMEC: human microvascular endothelial cells; HPAECs: human pulmonary arterial endothelial cells; EPC: endothelial progenitor cells; CMEC: cardiac microvascular endothelial cells; RBMEC: rat brain microvascular endothelial cells; ESC: embryonic stem cell; ECFC: circulating endothelial colony forming cells; EFNA3: Ephrin-A3; CUL2/3: cullin 2/3; Ets-1: v-ets erythroblastosis virus E26 oncogene homolog 1; GATA2: Endothelial transcription factor GATA2; PAK4: Serine/threonine-protein kinase PAK4; VE- cadherin: vascular endothelial (VE)-cadherin; VEGF: vascular endothelial growth factor; AGO1: argonaute 1; HBP1:HMG-box transcription factor 1; P21: cyclin dependent kinase inhibitor 1A; E2F-1/2: E2F transcription factor 1/2; P53: tumor protein p53; NRP1: Neuropilin 1; FAT4: FAT atypical cadherin 4; TBXA2R: thromboxane A2 receptor; PIK3R1: phosphoinositide-3-kinase regulatory subunit 1; RPS6KB1: ribosomal protein S6 kinase B1; HIF-1/2 $\alpha$ : hypoxia inducible factor 1/2 subunit alpha; STIM1: stromal interaction molecule 1; SPRED1: Sprouty-related protein; PIK3R2/p85 $\beta$ : phosphoinositol-3 kinase regulatory subunit 2; GABARAPL1: GABA type A receptor associated protein like 1; HMGB1: high mobility group box 1; TGF $\beta$ 2: transforming growth factor beta 2; EDNRB: endothelin receptor type B.

**Table 2. Endothelial angiogenesis associated miRNAs without AIS study.**

miRNA names	Cell types	miRNA target(s)	Impact on angiogenesis	References
miR-361	HUVEC	VEGF	inhibit	[25]
miR-29a	HUVEC	HBP1	promote	[26]
miR-31	EPC	FAT4;TBXA2R	promote	[22]
mir-223-3p	CMEC	RPS6KB1;HIF-1 $\alpha$	inhibit	[23]
miR-640	HUVEC	HIF-1 $\alpha$	inhibit	[27]
miR-193a-3p	ECFC	HMGB1	inhibit	[28]
miR-191	HUVEC	HIF-2 $\alpha$	inhibit	[24]
miR-503	EPC	Apelin	promote	[29]

Abbreviations: AIS: acute ischemic stroke; HUVEC: human umbilical vein endothelial cells; EPC: endothelial progenitor cells; CMEC: cardiac microvascular endothelial cells; ECFC: circulating endothelial colony forming cells; VEGF: vascular endothelial growth factor; HBP1:HMG-box transcription factor 1; FAT4: FAT atypical cadherin 4; TBXA2R: thromboxane A2 receptor; RPS6KB1: ribosomal protein S6 kinase B1; HIF-1/2 $\alpha$ : hypoxia inducible factor 1/2 subunit alpha; HMGB1: high mobility group box 1.

**Table 3. Characteristics of acute ischemic stroke and control subjects in Cohort A.**

Characteristic	Healthy controls (M $\pm$ SEM)	Stroke patients (M $\pm$ SEM)	P value
Age (years)	74.5 $\pm$ 3.9	71.3 $\pm$ 4.2	0.592
Gender (%)	50F/50M	50F/50M	1
CAD history, n(%)	2(33.3)	1(16.7)	1
HT history, n(%)	5(83.3)	3(50)	0.545
DM history, n(%)	2(33.3)	2(33.3)	1
Smoking history, n(%)	1(16.7)	1(16.7)	1
BMI(kg/m <sup>2</sup> )	26.8 $\pm$ 1.3	25.2 $\pm$ 0.6	0.297
SBP(mmHg)	145.7 $\pm$ 8.6	148.3 $\pm$ 7.5	0.820
DBP(mmHg)	73.5 $\pm$ 5.8	74.2 $\pm$ 3.6	0.204
mRS score	2.67 $\pm$ 0.8	-	-
HBA1c(%)	6.5 $\pm$ 0.5	6.8 $\pm$ 0.5	0.694
FBG(mmol/L)	5.7 $\pm$ 0.5	6.6 $\pm$ 0.6	0.307
TG(mmol/L)	1.3 $\pm$ 0.3	1.6 $\pm$ 0.6	0.719
TC(mmol/L)	4.4 $\pm$ 0.7	4.7 $\pm$ 0.5	0.789
LDL-C(mmol/L)	2.5 $\pm$ 0.5	2.8 $\pm$ 0.4	0.617
HDL-C(mmol/L)	1.6 $\pm$ 0.3	1.4 $\pm$ 0.2	0.732
Creatinine( $\mu$ mol/L)	80.3 $\pm$ 9.0	73.8 $\pm$ 7.1	0.584
BUN(mmol/L)	5.6 $\pm$ 0.4	6.2 $\pm$ 0.8	0.526
LP( $\alpha$ )(mg/L)	249.3 $\pm$ 120.1	288.3 $\pm$ 139.0	0.836
Hcy( $\mu$ mol/L)	15.8 $\pm$ 2.1	13.8 $\pm$ 0.8	0.341
AST(U/L)	18.4 $\pm$ 2.3	17.9 $\pm$ 1.5	0.861
ALT(U/L)	21.4 $\pm$ 3.0	16.6 $\pm$ 2.6	0.256
$\gamma$ GT(U/L)	41.8 $\pm$ 14.5	16.8 $\pm$ 1.7	0.118
CRP(mg/L)	2.4 $\pm$ 1.1	4.7 $\pm$ 3.0	0.481
WBC count( $\times 10^9$ /L)	5.7 $\pm$ 0.7	6.2 $\pm$ 0.6	0.605
Hemoglobin(g/L)	133.5 $\pm$ 6.3	139.3 $\pm$ 5.7	0.507
Platelets( $\times 10^9$ /L)	169.7 $\pm$ 13.3	177.8 $\pm$ 32.5	0.821
PT(s)	11.5 $\pm$ 0.6	10.5 $\pm$ 0.5	0.230
APTT(s)	33.1 $\pm$ 2.0	30.1 $\pm$ 2.0	0.311
FIB(g/L)	2.9 $\pm$ 0.2	3.0 $\pm$ 0.1	0.609

Abbreviations: CAD: coronary artery disease; HT: hypertension; DM: diabetes mellitus; BMI: body mass index; SBP: systolic blood pressure; DBP: diastolic blood pressure; HBA1c: glycolated hemoglobin A1c; FBG: fasting blood glucose; TG: total triglyceride; TC: total cholesterol; LDL-C: low density lipoprotein cholesterol; HDL-C: high density lipoprotein cholesterol; BUN: blood urea nitrogen; LP( $\alpha$ ): lipoprotein; Hcy: homocysteine; AST: aspartate aminotransferase; ALT: alanine aminotransferase;  $\gamma$ GT:  $\gamma$ -aminobutyric acid; CRP: C-reactive protein; WBC: white blood cell; PT: prothrombin time; APTT: activated partial thromboplastin time; FIB: fibrinogen.

**Table 4. Characteristics of acute ischemic stroke and control subjects in Cohort B.**

Characteristic	Healthy controls (M±SEM)	Stroke patients (M±SEM)	P value
Age (years)	75.4±2.8	75.3±3.0	0.968
Gender (%)	50F/50M	48.7F/51.3M	1
CAD history, n(%)	2(16.7)	2(16.7)	1
HT history, n(%)	8(66.7)	9(75)	1
DM history, n(%)	2(16.7)	3(25)	1
Smoking history, n(%)	3(25)	4(33.3)	1
BMI(kg/m <sup>2</sup> )	24.7±0.7	23.2±1.2	0.273
SBP(mmHg)	131.8±5.0	135.1±4.2	0.614
DBP(mmHg)	72.5±3.4	76.7±2.9	0.357
mRS	2.58±0.8	-	-
HBA1c(%)	5.8±0.2	5.9±0.8	0.838
FBG(mmol/L)	6.0±0.6	7.5±1.1	0.246
TG(mmol/L)	1.4±0.1	1.7±0.3	0.205
TC(mmol/L)	4.2±0.2	4.6±0.2	0.212
LDL-C(mmol/L)	2.7±0.2	2.9±0.2	0.411
HDL-C(mmol/L)	1.2±0.1	1.3±0.1	0.578
Creatinine(μmol/L)	82.8±8.8	88.8±8.6	0.631
BUN(mmol/L)	6.7±1.3	6.8±1.0	0.926
LP(α)(mg/L)	181.4±54.8	273.6±137.3	0.545
Hcy(μmol/L)	18.9±3.2	17.2±2.6	0.741
AST(U/L)	23.8±2.7	24.5±2.8	0.860
ALT(U/L)	20.3±2.6	20.0±2.8	0.925
γGT(U/L)	53.1±23.7	43.4±10.3	0.713
CRP(mg/L)	15.0±9.2	19.8±12.3	0.759
WBC count(×10 <sup>9</sup> /L)	7.0±0.9	6.9±1.1	0.890
Hemoglobin(g/L)	125.2±5.7	116.6±4.3	0.242
Platelets(×10 <sup>9</sup> /L)	177.3±17.2	262.9±59.0	0.177
PT(s)	12.5±1.0	11.4±0.2	0.317
APTT(s)	33.7±1.5	31.9±1.1	0.355
FIB(g/L)	3.2±0.2	4.0±0.6	0.256

Abbreviations: CAD: coronary artery disease; HT: hypertension; DM: diabetes mellitus; BMI: body mass index; SBP: systolic blood pressure; DBP: diastolic blood pressure; HBA1c: glycolated hemoglobin A1c; FBG: fasting blood glucose; TG: total triglyceride; TC: total cholesterol; LDL-C: low density lipoprotein cholesterol; HDL-C: high density lipoprotein cholesterol; BUN: blood urea nitrogen; LP(α): lipoprotein; Hcy: homocysteine; AST: aspartate aminotransferase; ALT: alanine aminotransferase; γGT: γ-aminobutyric acid; CRP: C-reactive protein; WBC: white blood cell; PT: prothrombin time; APTT: activated partial thromboplastin time; FIB: fibrinogen.

In contrast, transfection of cells with miR-191 inhibitor promoted tube formation (Figure 5B, 5D)

#### Function of miR-191 in HUVECs spheroid sprouting activity

We performed a 3-dimensional spheroid sprouting assay and demonstrated that over-expression of miR-191 significantly decreased the sprouting coverage area of HUVECs spheroids when compared with controls

(Figure 5E, 5G). In contrast, transfection of cells with miR191 inhibitor markedly enhanced the sprouting coverage area (Figure 5F, 5H).

#### Validation of predictive target gene of miR-191

Vascular endothelial zinc finger 1 (VEZF1) is one of the target genes of miR-191 predicted by TargetScan 7.2 and miRDB (Figure 6A). We found that VEZF1 mRNA levels were not influenced by miR-191 mimic or

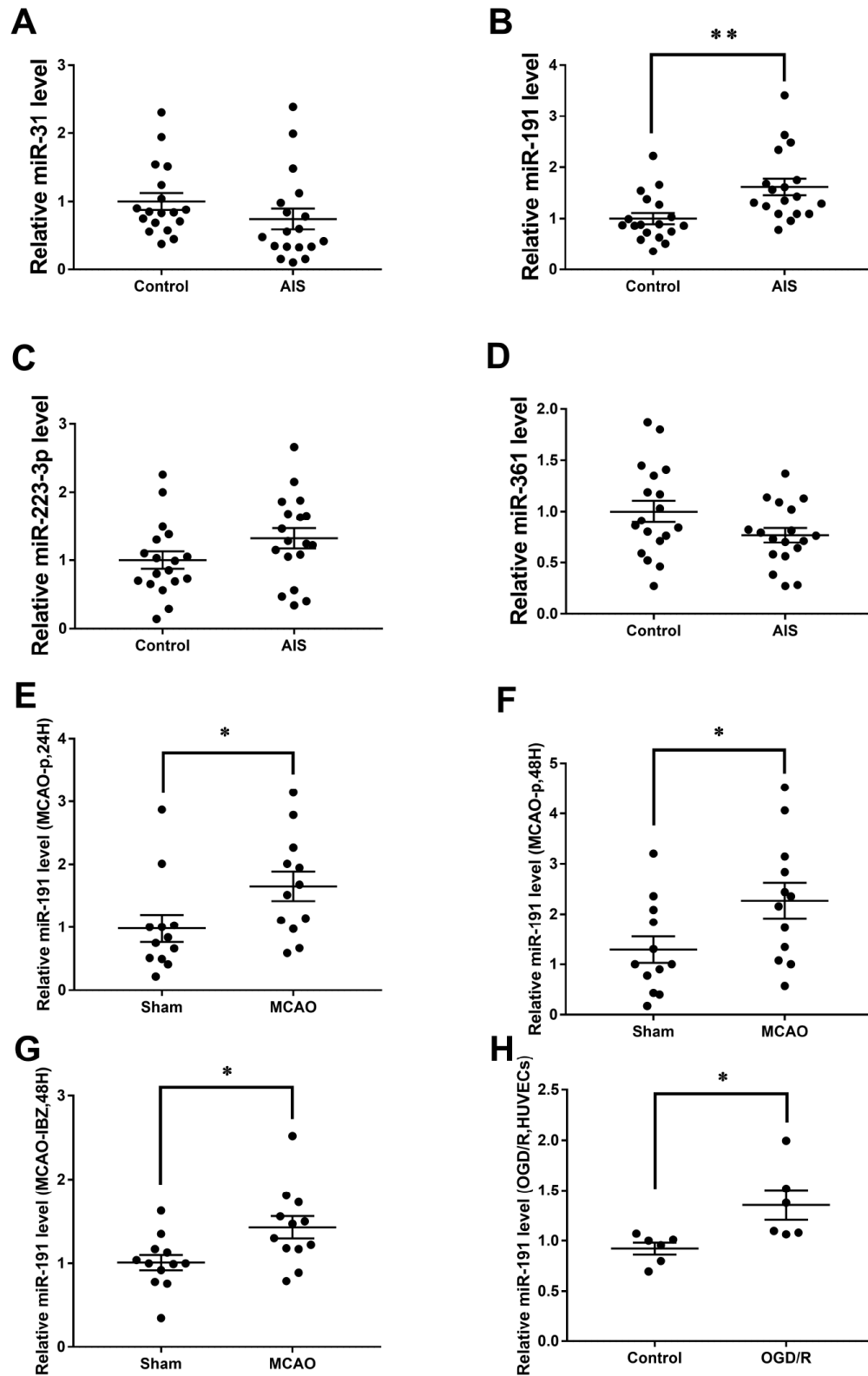


**Figure 1. Relative miRNAs levels.** Expression levels of miRNAs in Cohort A+B (n=18) (A) miR-31, (B) miR-191, (C) miR-223-3p, (D) miR-361; (E) Expression level of miR-191 in rat MCAO plasma after 24h reperfusion (n=12); (F) Expression level of miR-191 in rat MCAO plasma after 48h reperfusion (n=12); (G) Expression level of miR-191 in rat MCAO brains (n=12); (H) Expression level of miR-191 in OGD HUVECs (n=6). Means  $\pm$  SEM. \*  $P < 0.05$ , \*\*  $P < 0.01$  vs. NCM or NCI.

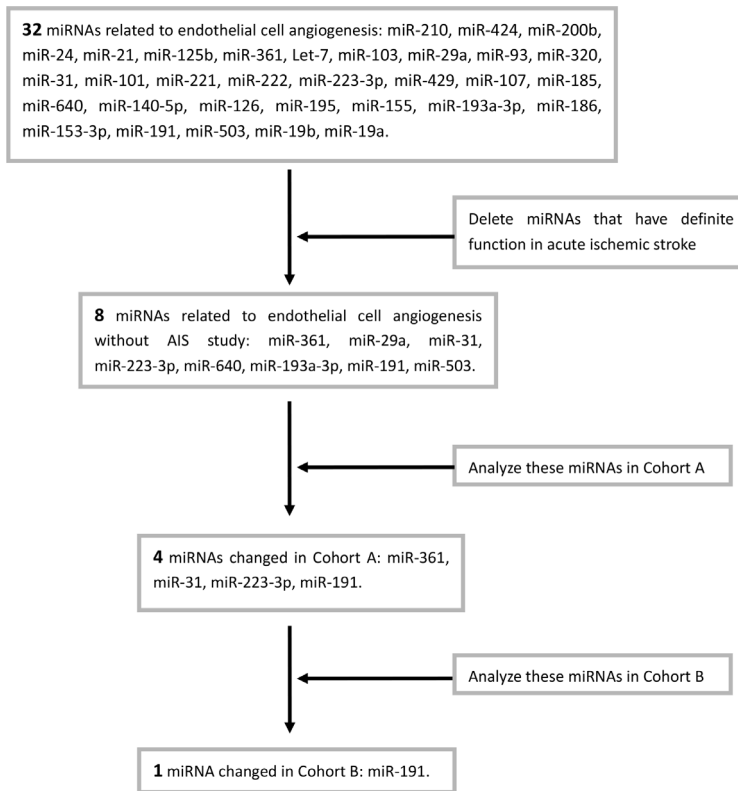
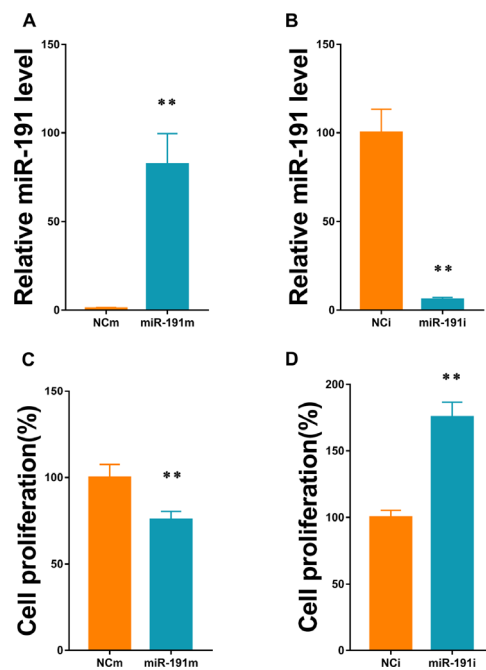


Chart 1. Screening process of miRNAs.



**Figure 2. MiR-191 transfection efficiency and cell proliferation.** (A, B) Expression level of miR-191 (in fold of NCm or percentage of NCI) in HUVECs that were transfected with miR-191 mimic (A) or miR-191 inhibitor (B) as assessed by real-time PCR (n=6 per group); (C, D) Proliferation (percentage of NCm or NCI) of HUVECs transfected with miR-191 mimic (C) or miR-191 inhibitor (D) as assessed by CCK-8 assay (n =6 per group). After transfection, the cells were reseeded into 96-well plates and incubated for another 48 h. Means  $\pm$  SEM. \*\* P< 0.01 vs. NCm or NCI.

miR-191 interference (Figure 6B). Since VEZF1 is a nucleus transcription factor, we then extracted nucleoprotein and found that over-expression of miR-191 decreased VEZF1 protein levels in nucleus, while miR-191 inhibitor increased the protein levels of VEZF1 (Figure 6C, 6D). Further luciferase assay showed a significant decrease in the luciferase activity of wild-type VEZF1 3' UTR (Figure 6E, 6F), indicating that VEZF1 is the target of miR-191.

### Action of miR-191 on VEZF1 signaling

VEZF1 has been reported to regulate several genes that are involved in angiogenesis, such as endothelin 1 (EDN1) [36], matrix metalloproteinase 2 (MMP2) [36], stathmin 1 (STMN1) [37], matrix metalloproteinase (MMPs) [38], Cbp/p300 interacting transactivator with Glu/Asp rich carboxy-terminal domain 2 (CITED2) [39]. In the present study, we found that miR-191 over-

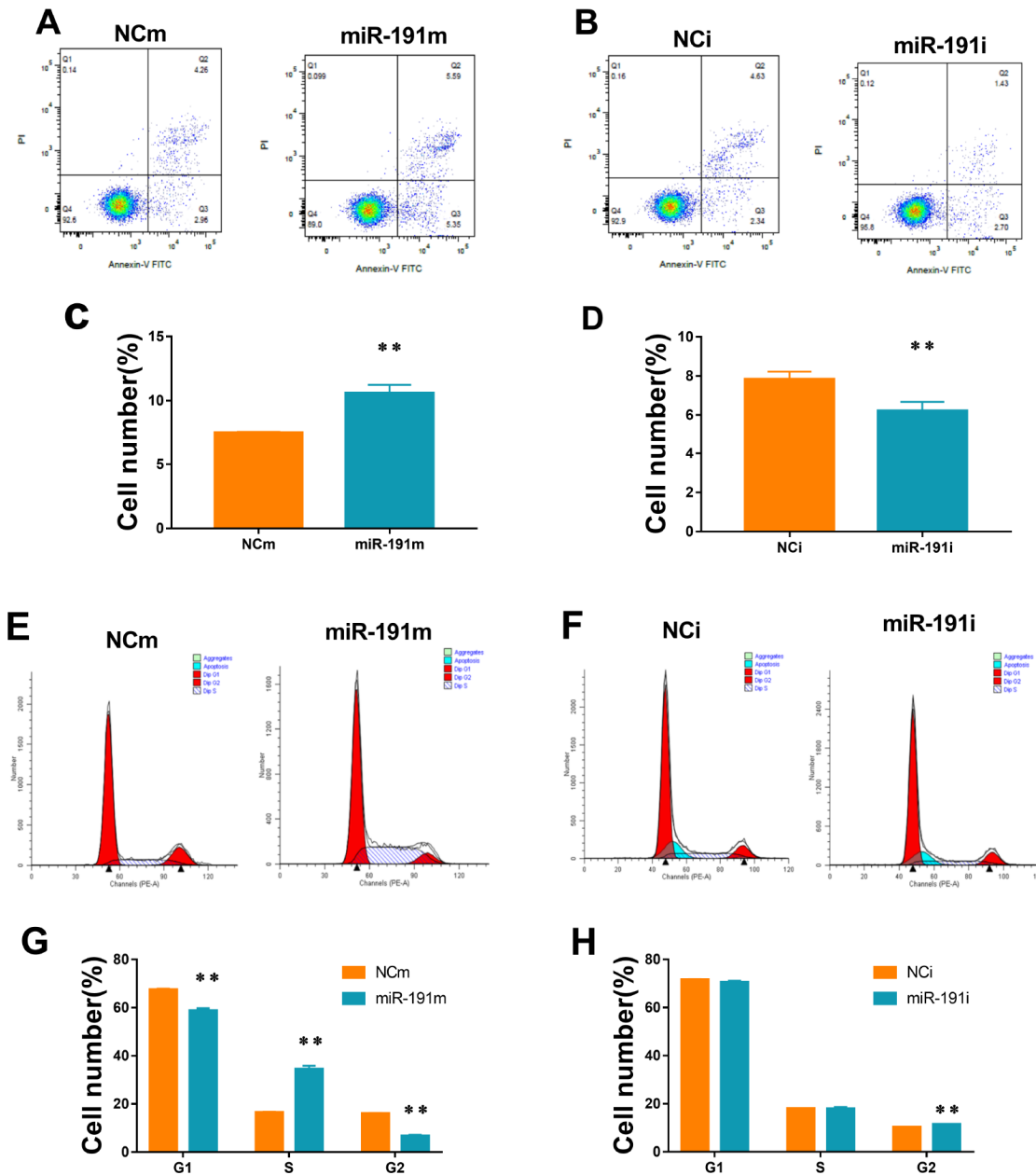


**Figure 3. Cell apoptosis and cell cycle.** (A, B) Cell apoptosis analysis of HUVECs transfected with miR-191 mimic (A) or miR-191 inhibitor (B) as assessed by flow cytometry; (C, D) Percentage of apoptosis HUVECs transfected with miR-191 mimic (C) or miR-191 inhibitor (D) (n=6 per group); (E, F) Cell cycle analysis of HUVECs transfected with miR-191 mimic (E) or miR-191 inhibitor (F) as assessed by flow cytometry; (G, H) Percentage of HUVECs transfected with miR-191 mimic (G) or miR-191 inhibitor (H) in different stages (n=6 per group). Means ± SEM, \*\* P<0.01 vs. NCm or NCi.



expression significantly suppressed the mRNA levels of EDN1, MMP1, and STMN1 and but increased the mRNA level of CITED2 (Figure 7A, 7C, 7E, 7G). Inhibition of miR-191 showed an opposite trend of the changes of these genes (Figure 7B, 7D, 7F, 7H). We did not find any effects of miR-191 on the mRNA levels of MMP2 and MMP9 (Figure 7I–7L).

### Inhibition of miR-191 reduced infarction volume of MCAO rats

The rats randomly received an intracerebroventricular infusion of miR-191/NC antagomir or blank control 3 days prior to MCAO. Compared to the NC antagomir, miR-191 antagomir significantly reduced the miR-191

levels both in plasma and IBZ at 48 h after reperfusion in MCAO rats (Figure 8A, 8B). We found that VEZF1 mRNA levels of IBZ were not influenced by miR-191 antagomir (Figure 8C) which was consistent with the results of cell experiments. However, the protein levels of VEZF1 were increased significantly (Figure 8D, 8E). We also found that rats receiving miR-191 antagomir had smaller brain infarct volumes than those with NC antagomir (Figure 8F, 8G).

## DISCUSSION

Impaired angiogenesis plays a crucial role in cerebral injury after acute ischemic attack [6]. MiRNAs have been shown to be important regulators involved in the

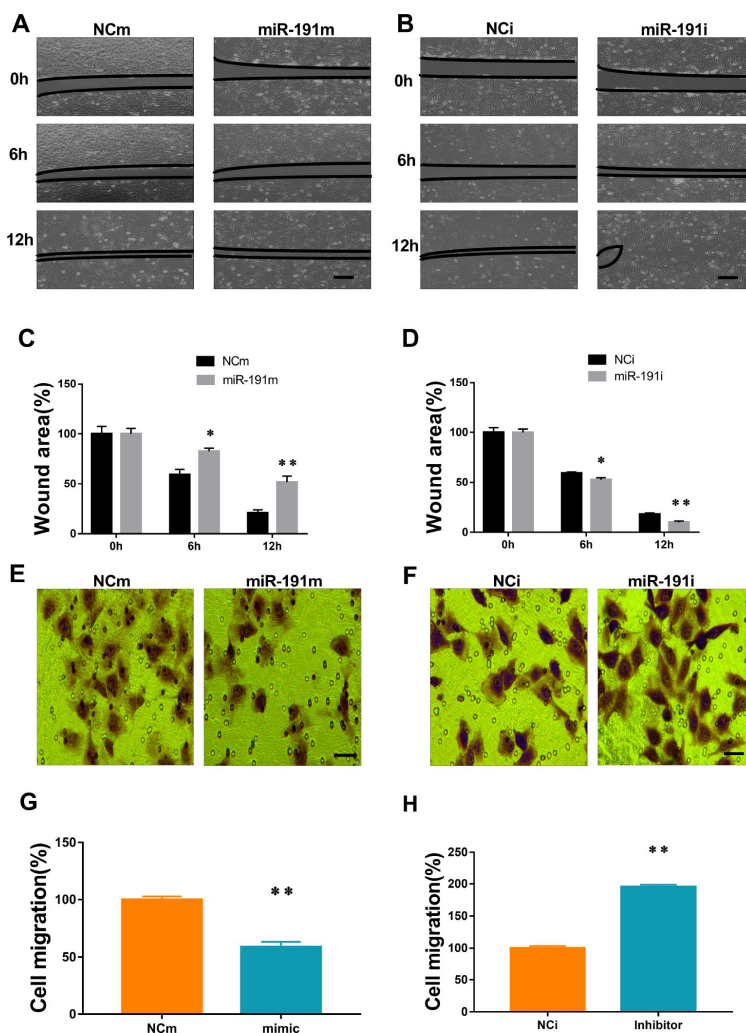


**Figure 4. MiR-191 inhibited cell migration.** (A, B) Phase contrast microscopic images of HUVECs at 0, 6, and 12 h after scratching. The cells were transfected with miR-191 mimic (A), miR-191 inhibitor (B), or the corresponding scrambled NCm (A) and NCI (B). Black lines indicate the wound area. Scale bars, 100  $\mu$ m. (C, D) Size of wound area (percentage of 0 h) created by scratching HUVECs transfected with miR-191 mimic (C) or miR-191 inhibitor (D) (n = 6 per group). (E, F) Phase contrast microscopic images of HUVECs migrated and attached to the bottom membrane of a transwell. The cells were transfected with miR-191 mimic (E), miR-191 inhibitor (F), or the corresponding scrambled NCm (E) and NCI (F). Scale bars, 20  $\mu$ m. (G, H) Number of migrated HUVECs (percentage of NCm or NCI) transfected with miR-191 mimic (G) or miR-191 inhibitor (H) (n = 6 per group). Means  $\pm$  SEM. \* P < 0.05, \*\* P < 0.01 vs. NCm or NCI.

process of angiogenesis [10, 40]. Here we showed for the first time that miR-191 was elevated in the plasma of AIS patients as well as in MCAO rat model and OGD/R HUVEC model. Over-expression of miR-191 promoted apoptosis but inhibited proliferation, migration, tube-forming and spheroid sprouting activity in HUVECs, while silence of miR-191 displayed opposite results. Mechanistically, we found that miR-191 directly regulated VEZF1, leading to the changes of a variety of angiogenesis-associated genes targeted by VEZF1. *In vivo* studies demonstrated that inhibition of miR-191 could reduce the infarction volume induced by

MCAO in rats. Therefore, miR-191 might be a novel therapeutic target for the treatment of AIS.

Angiogenesis is one of the key repair mechanisms for the ischemic injury induced by acute stroke [7]. Gu *et al.* [35] demonstrated that miR-191 was preferentially expressed in endothelial cells compared to other types of human cells and displayed antiangiogenic effect. In the present study, we performed a series of well-established angiogenesis assays and demonstrated that miR-191 is an inhibitor of angiogenesis with effects of suppressing proliferation, migration, tube formation and spheroid

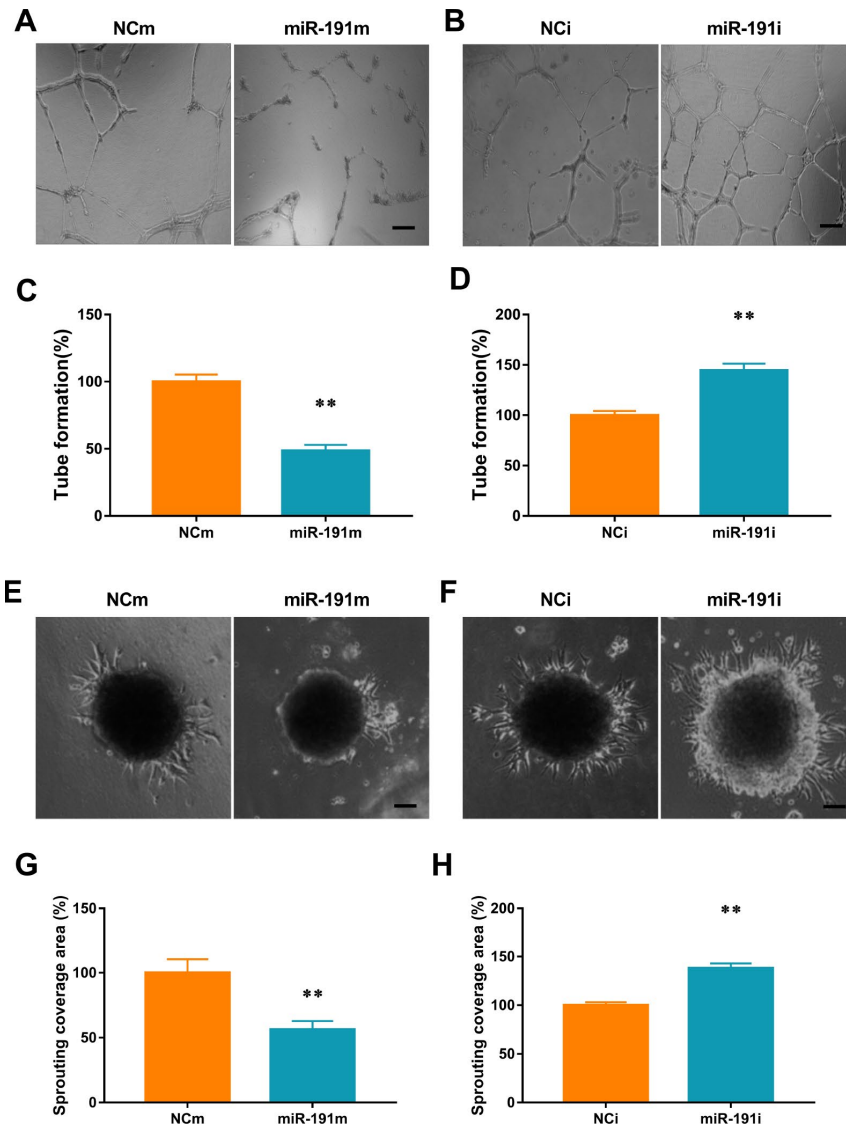


**Figure 5. miR-191 inhibited tube formation and spheroid sprouting.** (A, B) Phase-contrast microscopic images of tube-forming HUVECs that were transfected with miR-191 mimic (A), miR-191 inhibitor (B), or the corresponding scrambled NCm (A) and NCi (B). Scale bars, 20µm. (C, D) Tube formation of HUVECs (percentage of NCm or NCi) transfected with miR-191 mimic (C) or miR-191 inhibitor (D) as assessed by tube formation assay (n = 6 per group). (E, F) Phase-contrast microscopic images of sprouting HUVECs spheroids. HUVECs were transfected with miR-191 mimic (E), miR-191 inhibitor (F), or the corresponding scrambled NCm (E) and NCi (F). Scale bars, 20µm. (G, H) Sprouting coverage area of HUVECs (percentage of NCm or NCi) transfected with miR-191 mimic (G) or miR-191 inhibitor (H) as assessed by spheroid sprouting assay (n = 6 per group). Means ± SEM. \*\* P < 0.01 vs. NCm or NCi.

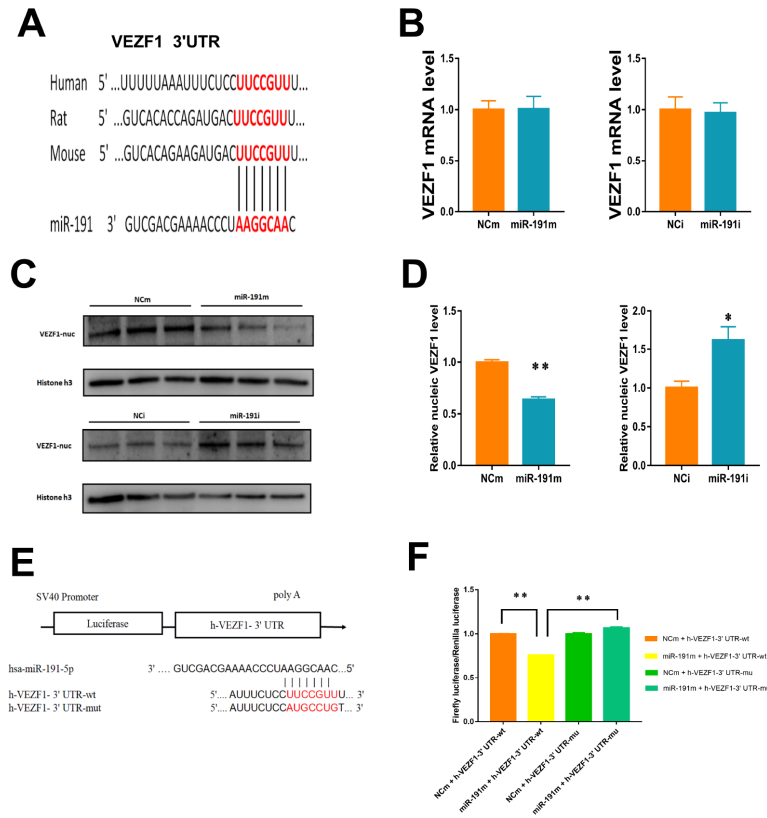


**Figure 6. Regulation of VEZF1 by miR-191.** (A) MiR-191 and its putative binding sequence in the 3'-UTR of VEZF1. (B) Real-time PCR analysis of VEZF1 expression in HUVECs by miR-191 interference. (n = 6 per group); (C, D) Western blot analysis of VEZF1 expression in HUVECs transfected by miR-191. (E) Construction of Plasmid; (F) Luciferase activities were measured to evaluate the binding of miR-191 to the candidate binding sequence of VEZF1 after transfection of miR-191 mimic or NCm. Means  $\pm$  SEM. \*  $P < 0.05$ , \*\*  $P < 0.01$  vs. NCm or NCi.

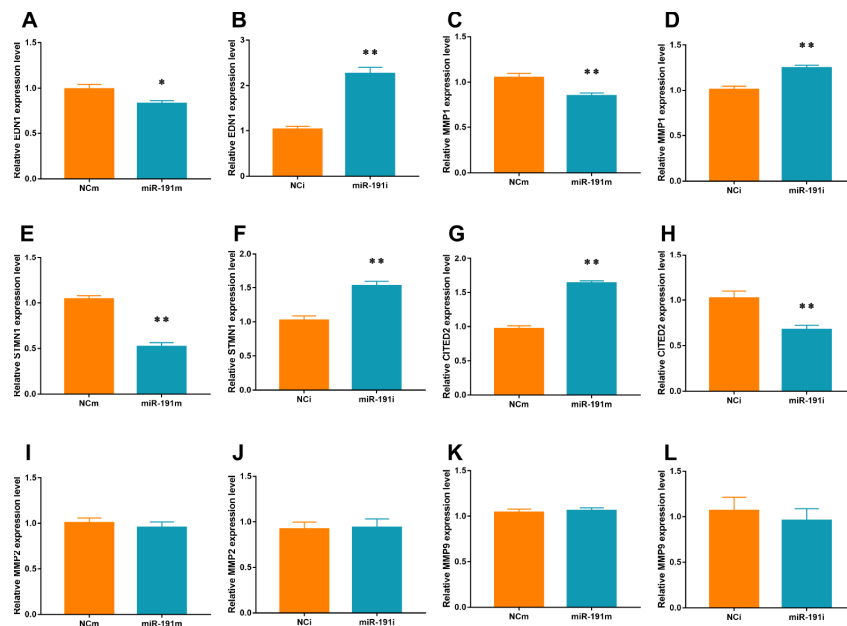


**Figure 7. mRNA levels of Targets of VEZF1.** Real-time PCR for EDN1 (A, B), MMP1 (C, D), STMN1 (E, F), CITED2 (G, H), MMP2 (I, J), and MMP9 (K, L) mRNA of HUVECs transfected with miR-191 mimic or miR-191 inhibitor (n = 6 per group). Means  $\pm$  SEM. \*  $P < 0.05$ , \*\*  $P < 0.01$  vs. NCm or NCi.

sprouting in HUVECs. Knockdown of miR-191 could reduce the infarction area induced by MCAO in rats and promote proliferation, migration, tube formation and spheroid sprouting in HUVEC. Our results complement nicely with a previous report showing that knockout of miR-191 reduced hepatic ischemia-reperfusion injury through inhibiting inflammatory responses and cell death [41]. Another study also showed that up-regulated miR-191 participated in renal ischemia-reperfusion injury via inducing apop-

tosis of renal tubular epithelial cells [42]. These results indicate that lowering miR-191 might be a potential therapy for ischemia-reperfusion injury. However, although we found that plasma levels of miR-191 were increased in patients with AIS, there might be false positive and negative results in the process of miRNA screening because of the relative small sample size. Future studies with larger sample size will be needed to verify the exact roles of miR-191 in the diagnosis and prediction of AIS.

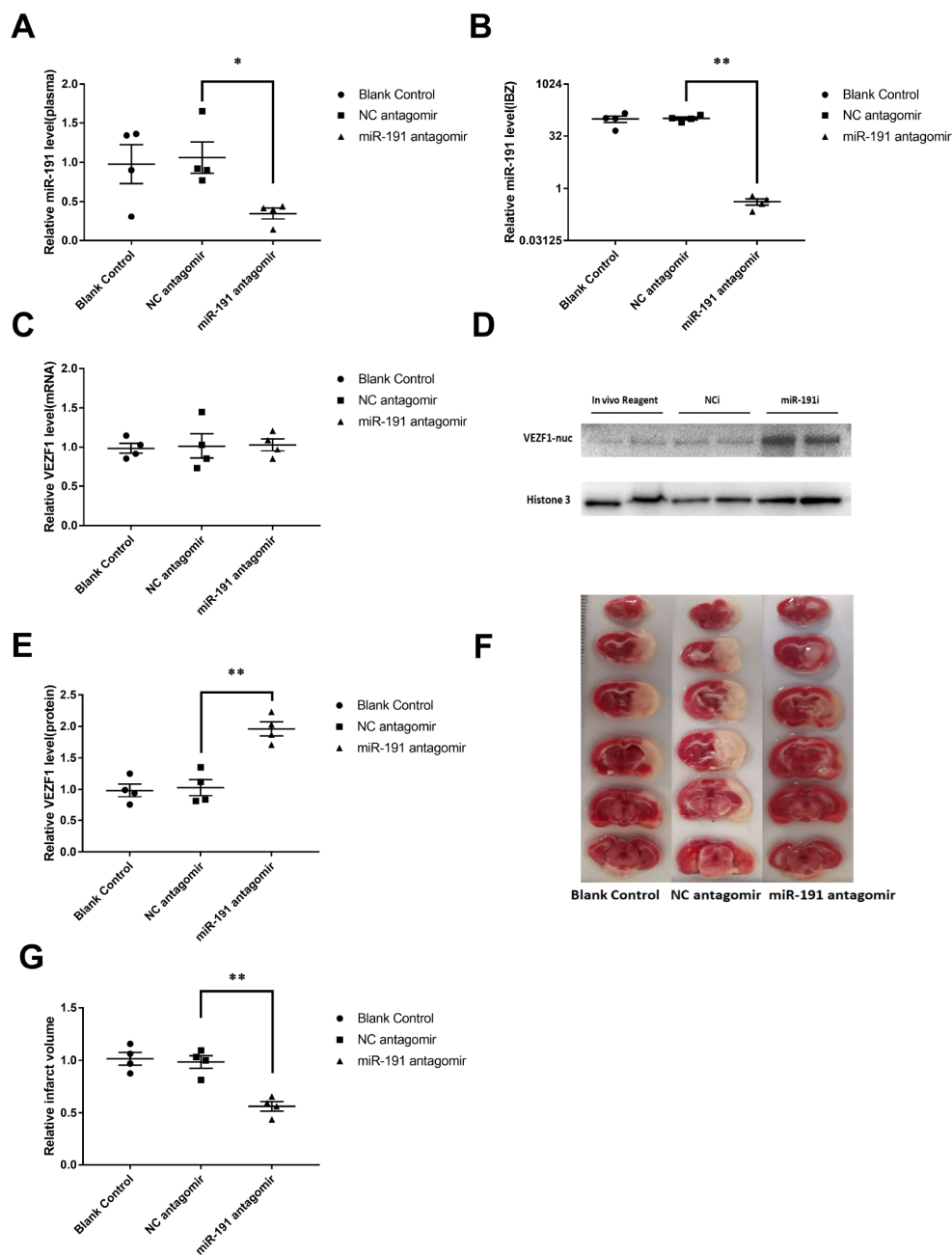


**Figure 8. Inhibition of miR-191 reduced infarction volume of MCAO rats after the injection of miR-191 antagonist compared to NC antagonist and blank control.** Relative miR-191 levels in (A) plasma and (B) IBZ (n =4 per group); (C) Real-time PCR analysis of VEZF1 expression in IBZ (n =4 per group); (D, E) Western blot analysis of VEZF1 expression in IBZ (n =4 per group); (F, G) Relative infarct volume of MCAO rats (n =4 per group). Means  $\pm$  SEM. \* P < 0.05, \*\* P < 0.01 vs. NC antagonist.

VEZF1 encodes a zinc finger transcription factor which is essential for developmental angiogenesis and lymphangiogenesis. Mammalian VEZF1 is expressed in the anterior-most mesoderm at E7.5 during development and is later restricted in the vascular endothelium [43]. VEZF1 knockout mice showed embryonic lethality caused by vascular remodeling defects and loss of vascular integrity, indicating that VEZF1 is a critical regulator of vascular development [44]. VEZF1 is thus proposed to act as a transcriptional activator of pro-angiogenic genes including EDN1 [36], MMP2 [36], STMN1 [37], MMPs [38], CITED2 [39]. VEZF1 can be epigenetically regulated by histone acetylation and deacetylation [43]. VEZF1 is specifically expressed in endothelial cells and correlated with the differentiation and proliferation of endothelial cells in the embryonic vascular system [45]. A series of studies showed that VEZF1 could activate angiogenesis by promoting endothelial cells proliferation, migration and vessel network formation [37, 39, 46, 47]. Our data demonstrated that VEZF1 is regulated by miR-191 at post-translational level. Luciferase reporter assay validated that VEZF1 is a direct target of miR-191. To further prove miR-191 inhibit HUVECs angiogenesis by targeting VEZF1, we measured the expression levels of the VEZF1 targets [36–39] after miR-191 interference. Our data shown that over-expression of miR-191 inhibited the expression of angiogenesis-related genes including EDN1, MMP1, and STMN1. However, further intervention studies are needed to elucidate whether miR-191 inhibited angiogenesis via targeting VEZF1.

In conclusion, our data reveal a novel role of miR-191 in promoting ischemic brain injury through inhibiting angiogenesis via targeting VEZF1, which in turn resulted in up-regulation of CITED2 and down-regulation of MMP-1, STMN1.(Figure 9). MiR-191 might be served as a promising effective biomarker and therapeutic target for AIS.

## METHODS

### Ethics statement

Investigation was conducted in accordance with the ethical standards and according to the Declaration of Helsinki and was approved by the Ethics Committee of Sir Run Run Hospital, Nanjing Medical University (Protocol Numbers: 2018-SR-25, Supplementary Figure 2) and the Animal Ethical and Welfare Committee of Nanjing Medical University (Protocol Numbers: IACUC-1806010, Supplementary Figure 3).

### Patient enrollment

Patients were recruited consecutively from the department of geriatrics of Sir Run Run Hospital, Nanjing Medical University from January to June 2018. There were total 18 patients with AIS and 18 controls. AIS patients were recruited from stroke center within six hours from the onset of the symptoms before thrombolytic therapy. AIS diagnosis was confirmed using clinical features and brain MRI by two investigators in a double-blinded manner according to the 2018 Guidelines for the Early Management of Patients With Acute Ischemic Stroke [2]. The control subjects were selected during the same period in the same hospital from the health examination center. Exclusion criteria including: under 18 or over 90 years old; history of intracranial hemorrhage; craniocerebral trauma; giant intracranial aneurysms; recent (within 3 months) history of intracranial surgery; malignant tumors. Informed consents were obtained from all subjects.

### MCAO

Male Sprague Dawley rats (7-8w, 230 g–280 g) randomly divided into two groups (12 in each group) were obtained from Shanghai Sippr-BK laboratory animal Co. Ltd. Right MCAO was induced using an intraluminal filament as Longa, E.Z. *et al* [48] described. The body temperature was maintained at 37 °C with a homothermal blanket and physiological parameters were monitored during the surgical procedure. After anesthetized with 1 % pentobarbital sodium (0.5ml/100g), the right common carotid artery (CCA), external carotid artery (ECA) and internal

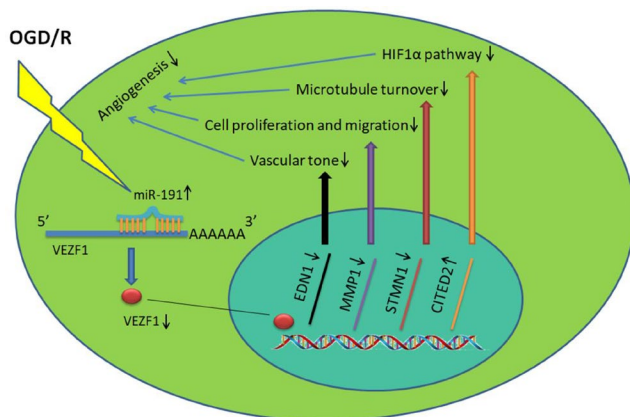


**Figure 9. miR-191 reduces the nucleoprotein VEZF1, resulting in up-regulation of CITED2 and down-regulation of MMP-1, STMN1 mRNA.** This, in turn, suppresses HUVEC proliferation and migration and thus prevents endothelial tube formation and spheroid sprouting. Moreover, miR-191 suppresses the expression of EDN1 which functions as maintaining vascular tension.

carotid artery (ICA) were sequentially isolated. An incision was made in the distal region of the CCA, then a 40mm long (diameter: 0.26-0.28mm) poly-L-lysine coated nylon monofilament (Beijing Shadong Biotechnology Co., Ltd.) was inserted into the ICA, and the monofilament was advanced approximately 18-20mm beyond the carotid bifurcation until mild resistance was encountered. The occlusion was sustained for 2 h. The sham group underwent similar procedures, but the monofilament was not advanced into the CCA.

Neurological evaluations were performed according to an established graded scoring system at 24 h after reperfusion to verify the modeling success in function [49]. Briefly, neurological deficits were scored as follows: 0, no deficit; 1, failure to extend left forepaw upon lifting the whole animal by tail; 2, grip strength weakening of the left forepaw; 3, circling to the left when held by the tail; and 4, spontaneous circling.

Peripheral venous blood was collected at 24 and 48 hours after reperfusion and the brains were removed and frozen at  $-20^{\circ}\text{C}$  for 15 min at 48 hours after reperfusion when sacrificed (Supplementary Figure 3). To histologically verify the success of the model, coronal sections were cut into 2 mm thick slices, stained with 1% 2,3,5-triphenyltetrazolium chloride (TTC) at  $37^{\circ}\text{C}$  in the dark for 20 min, and photographed (Supplementary Figure 4).

#### **Plasma and brain fragments collection and storage**

Peripheral blood samples were collected in tubes anticoagulated with ethylenediamine tetraacetic acid (EDTA) dipotassium salt after a definite diagnosis before any medication is administered. The samples were centrifuged ( $1000\times g$ , 5 minutes,  $4^{\circ}\text{C}$ , Beckman Coulter) to remove blood cells and debris, and then transferred to 1.5ml microtubes (Axygen, MCT-150-C) for storage at  $-80^{\circ}\text{C}$  until further processing. Brain fragments were collected and stored in liquid nitrogen.

#### **Primary HUVECs isolation and culture**

Fresh umbilical cords were obtained following delivery of healthy babies to healthy mothers. HUVECs were isolated from umbilical cords according to a previously described method [50]. Briefly, the umbilical vein was inserted an intravenous needle for single use with tube and flushed with 30ml  $37^{\circ}\text{C}$  phosphate buffer saline (PBS), following which the cord was clamped at the distal end and the vessel filled with collagenase (Type Ia, 1 mg/mL, Sigma, C9891), until mildly distended. Following incubation at  $37^{\circ}\text{C}$  for 10-15 min, the cord was unclamped and the digest drained. The vessel was

gently massaged and flushed through with 20ml endothelial cell medium (ECM, Science, 1001), and the digests were pooled. The endothelial cell suspension was centrifuged ( $500\times g$ , 5 min), and the cell pellet was resuspended in ECM. This suspension was seeded into a 25ml flask (Corning, 430639).

The cells were incubated at  $37^{\circ}\text{C}$ , 5%  $\text{CO}_2$  until they are 85% - 90% confluent. Then, cells were detached from the substratum by exposure to 0.25% trypsin-EDTA (Gibco, 25200072, US) for 1 min at  $37^{\circ}\text{C}$ , pelleted ( $500\times g$ , 5 min) and passaged at a ratio of 1:3-5. Confluent cells at passage 3-6 were used for all experiments.

#### **OGD/R**

The OGD/R protocol was performed to mimic ischemia *in vitro*. Briefly, culture medium was removed and rinsed with PBS for three times. HUVECs were placed into a tri-gas incubator (memmert, Eastern Friesland, Germany) containing 1%  $\text{O}_2$ , 5%  $\text{CO}_2$ , 94%  $\text{N}_2$  at  $37^{\circ}\text{C}$  with glucose-free Dulbecco's Modified Eagle Medium (DMEM, Gibco, 11966025, US). After two hours challenge, DMEM was replaced with ECM. The cells were maintained for further 24 h at  $37^{\circ}\text{C}$  in a humidified 5%  $\text{CO}_2$  incubator to generate reperfusion.

#### **Total RNA isolation**

Total RNA was isolated from plasma, brain and cell samples using TRIzol (CWBio, CW0580) reagent following the manufacturer's instructions. RNA concentration and purity were determined with one drop spectrophotometer (OD-1000+, Nanjing wuyi Science and Technology Co., Ltd., China).

#### **Quantitative real-time polymerase chain reaction (qRT-PCR)**

CDNA was generated from 1  $\mu\text{g}$  RNA using miRNA 1st Strand cDNA Synthesis Kit (by stem-loop) (vazyme, MR101-02, Nanjing, China) for miRNA or PrimeScript<sup>TM</sup> RT reagent Kit (Perfect Real Time) (Takara, RR047A, Japan) for mRNA. Real-time PCR was performed using QuantStudio 5 (Applied Biosystems, US) with miRNA Universal SYBR qPCR Master Mix (vazyme, MQ101-02) for miRNA or Maxima SYBR Green/ROX qPCR Master Mix (2X) (Thermo Scientific<sup>TM</sup>, K0221, US) for mRNA according to the manufacturer's protocol. All reactions were run in triplicate and relative gene expression was calculated using the comparative threshold cycle (Ct) method (relative gene expression =  $2^{-(\Delta\text{Ct}_{\text{sample}} - \Delta\text{Ct}_{\text{control}})}$ ). The U6 snRNA was used as an internal control for miRNA while TATA-binding protein (TBP) used for mRNA. The gene-specific primers sequences are listed in Table 5.

**Table 5. Primer sets for real-time PCR analyses.**

<b>Gene</b>	<b>Forward primer (5' to 3')</b>	<b>Reverse Primer (5' to 3')</b>
U6 (MIM:180692)	CTCGCTTCGGCAGCACA	AACGCTTCACGAATTTGCGT
TBP (NM_003194)	CCACTCACAGACTCTCACAAC	CTGCGGTACAATCCCAGAACT
VEZF1 (NM_007146)	GGACAGCTATCACCTGAGGC	GCGATGGTAGAGATAAGGGGAA
MMP1 (NM_002421)	AAAATTACACGCCAGATTTGCC	GGTGTGACATTACTCCAGAGTTG
MMP2 (NM_004530)	TACAGGATCATTGGCTACACACC	GGTCACATCGCTCCAGACT
MMP9 (NM_004994)	TGTACCGCTATGGTTACTCTCG	GGCAGGGACAGTTGCTTCT
EDN1 (NM_001168319)	AGAGTGTGTCTACTTCTGCCA	CTTCCAAGTCCATACGGAACAA
CITED2 (NM_006079)	CCTAATGGGCGAGCACATACA	GGGGTAGGGGTGATGGTTGA
STMN1 (NM_203401)	TCAGCCCTCGGTCAAAGAAT	TTCTCGTGCTCTCGTTTCTCA

<b>miRNA</b>	<b>Accession</b>	<b>Reverse transcription primers (5' to 3')</b>	<b>Forward primers (5' to 3')</b>
miR-29a	MIMAT0004503	GTCGTATCCAGTGCAGGGTCCGAGGTATT CGCACTGGATACGACCTGAAC	GCGCGACTGATTTCTTTTGT GT
miR-31	MIMAT0000089	GTCGTATCCAGTGCAGGGTCCGAGGTATT CGCACTGGATACGACAGCTAT	GCGAGGCAAGATGCTGGC
miR-138	MIMAT0000430	GTCGTATCCAGTGCAGGGTCCGAGGTATT CGCACTGGATACGACCGGCT	GCGAGCTGGTGTGTGAAT C
miR-191	MIMAT0000440	GTCGTATCCAGTGCAGGGTCCGAGGTATT CGCACTGGATACGACCAGCTG	CGCAACGGAATCCCAAAA G
miR-193a-3p	MIMAT0000459	GTCGTATCCAGTGCAGGGTCCGAGGTATT CGCACTGGATACGACTGGG	CGCGAACTGGCCTACAAAG T
mir-223-3p	MIMAT0000280	GTCGTATCCAGTGCAGGGTCCGAGGTATT CGCACTGGATACGACTGGGGT	GCGCGTGTGAGTTTGTCAA AT
miR-361	MIMAT0000703	GTCGTATCCAGTGCAGGGTCCGAGGTATT CGCACTGGATACGACGTACCC	GCGCGTTATCAGAATCTCC AG
miR-503	MIMAT0002874	GTCGTATCCAGTGCAGGGTCCGAGGTATT CGCACTGGATACGACCTGCAG	CGTAGCAGCGGGAACAGTT
miR-640	MIMAT0003310	GTCGTATCCAGTGCAGGGTCCGAGGTATT CGCACTGGATACGACAGAGGC	CGCGATGATCCAGGAACCT

Abbreviation: TBP: TATA-box binding protein; MMP1/2/9: matrix metalloproteinase 1/2/9; EDN1: endothelin 1; CITED2: Cbp/p300 interacting transactivator with Glu/Asp rich carboxy-terminal domain 2; STMN1: stathmin 1.

## **Transfection of miR-191 mimic or inhibitor into HUVECs**

The cells were transfected for 24 h with 50 nM miR-191 mimic (Ribobio, Guangzhou, China) or 100 nM miR-191 inhibitor (Ribobio) using Lipofectamine 3000 (Invitrogen, US) according to the manufacturer's protocol. Cells transfected with negative control of mimic (NCm) (Ribobio) or negative control of inhibitor (NCi) (Ribobio) served as controls.

## **Cell proliferation assay**

To assess the proliferation rate of HUVECs, Cell Counting Kit-8 (CCK-8) assays (Dojindo, Japan) were performed according to the manufacturer's instructions. Briefly, 3000 HUVECs in 100  $\mu$ l of cell suspension were seeded in 96-well flat-bottomed plates. After 8 hours incubation, CCK-8 reagent was added to each well, and the absorbance of each well was measured at 450 nm after 3 hours incubation by a microplate reader (Synergy H1, BioTek, US). A value of 100% was assigned to the respective control group.

## **Flow cytometric analysis of apoptosis**

HUVECs were treated with miR-191 mimic/inhibitor for 24 h, and then subjected to OGD/R for 2 h/18 h. The apoptotic cell death rate was examined with Annexin V-FITC and PI double staining using the Annexin V-FITC apoptosis detection kit (Beyotime Biotechnology, C1063, Shanghai, China) according to the manufacturer's instructions. Briefly,  $5 \times 10^4$  cells were collected with 0.25% EDTA free trypsin (Gibco, 15050065, US), washed and resuspended in PBS. After staining with Annexin V-FITC/PI, flow cytometric analysis was performed and data were analyzed using FlowJo software.

## **Flow cytometric analysis of cell cycle**

HUVECs were treated with miR-191 mimic/inhibitor for 24 h, and then subjected to OGD/R for 2 h/18 h. HUVECs were collected and fixed in 70% ethanol overnight at 4 °C by using the cell cycle detection kit (KeyGen BioTech, KGA512, Jiangsu, China). Single-cell suspensions were labeled with PI for 30 min at 4 °C and analyzed by flow cytometry (BD, New York, US). The data were analyzed with FlowJo software.

## **Cell migration assay**

Scratch wound healing assay and transwell migration assay were performed to evaluate the motility of HUVECs. For the scratch wound healing assay,  $5 \times 10^5$  of HUVECs were seeded in a 6-well plate. After reaching confluence, the cell monolayer was scratched

with a pipette tip (10  $\mu$ l) to generate 4 scratch wounds and then rinsed twice with PBS to remove nonadherent cells. Phase-contrast light micrographs were taken immediately after scratching (0 h) as well as after 6 h and 12 h with  $\times 200$  magnification using a CKX41 microscope (Olympus, Japan).

For the transwell migration assay,  $2 \times 10^5$  of HUVECs in 500  $\mu$ l 1% FBS ECM were seeded into a 24-well insert (costar, 3422), and 750  $\mu$ l of 15% FBS ECM was added to the lowerwell. After 24h of incubation, nonmigrated cells were removed with cotton swabs, and migrated cells were stained with 0.1% crystal violet (Solarbio, C8470, Beijing, China). The number of migrated cells was determined in 3 microscopic regions of interest at  $\times 200$  magnification using a CKX41 microscope.

## **Tube formation assay**

To analyze the function of miR-191 in the tube-forming activity of HUVECs, 50  $\mu$ l of Matrigel (8-12mg/ml; Corning) was plated in each well of a 96-well plate. After Matrigel polymerization,  $3 \times 10^4$  of HUVECs in 100  $\mu$ l ECM were added into each well. After 12 h, vessel-like network structures were examined under CKX41 microscope. Tube formation was quantified by measuring the number of meshes using ImageJ software [National Institutes of Health (NIH), Bethesda, MD, USA].

## **Spheroid sprouting assay**

HUVECs were suspended in ECM containing 0.25% (w/v) methylcellulose (Sigma-Aldrich) and seeded (1000 cells/100  $\mu$ l) in low attachment, round-bottom, 96-well spheroid microplates (Corning, 4520). After incubation for 24 h, spheroids were harvested and resuspended in 20  $\mu$ l Matrigel. The spheroid-containing Matrigel was rapidly transferred to 24-well plates and allowed to polymerize for 30 min, after which 500  $\mu$ l ECM was added to each well. After 24h of incubation, the spheroid-sprouting capacity was quantified by measuring the sprouting coverage area of the sprouts using imageJ software.

## **Luciferase reporter assays**

293T cells ( $3 \times 10^5$  cells per well) were plated onto 24-well plates. pSV40-VEZF1-wt or pSV40-VEZF1-mut was cotransfected with miRNA-191 mimic or NCm into 293T cells by Lipofectamine 3000. The relative luciferase activity was normalized to Renilla luciferase activity 48h after transfection.

## **Protein extraction and Western blots**

Nuclear extracts were prepared with NE-PER™ Nuclear and Cytoplasmic Extraction Reagents according to the



manufacturer's protocol (Thermo Scientific, 78833, US). Protein concentrations were measured by BCA protein assay (Beyotime Biotechnology, Shanghai, China). Equal amounts (20 µg) of protein were separated by 4-20% GenScript SurePAGE, Bis-Tris, precast polyacrylamide gels (GenScript Biotechnology, Nanjing, China) electrophoresis and transferred to polyvinylidene fluoride membranes (Millipore, Billerica, MA, USA). Membranes were then incubated overnight at 4 °C with a 1:1000 dilution of anti-Histone H3 (Cell Signaling Technology, 4499s, US) and anti-VEZF1 (Proteintech, 19003-1-AP, US). After additional incubation with a 1:5000 dilution of anti-rabbit IgG (heavy and light chain) antibody (CST, 7074S) for 2 h, the immune complexes were detected by Immobilon Western HRP Substrate Peroxide Solution (Millipore Corporation, Billerica, MA 01821, USA). And images were acquired using ChemiDoc™ XRS+ Imaging System (Bio-rad, US). The intensity of immunoreactivity was assessed using Image Lab 6.0 software.

### **Intracerebroventricular injection of the miR-191 antagomir**

The miR-191 antagomir and NC antagomir were purchased from RiboBio(Guangzhou, China). The NC and miR-191 antagomir (2.5 µg/2.5 µl) were diluted with 1.25 µl of Entranster™ in vivo transfection reagent (Engreen,18668-11-1, Beijing, China). The solution was mixed with 1.25µl PBS gently, kept at room temperature for 5 min and then injected intra-cerebroventricularly (i.c.v.) using a microsyringe (KD Scientific Inc., USA) under the guidance of a stereotaxic instrument (RWD Life Science). A solution of 3.75µl PBS added with 1.25 µl of Entranster™ in vivo transfection reagent was acted as blank control. Intracerebroventricular injection was performed according to a previously described method [51]. The stereotaxic coordinates the right lateral ventricle: ML: -1.40mm, AP: -0.36mm, DV: -3.90mm.

### **Statistics**

Differences between the two groups were analyzed by the unpaired Student's *t* test or Mann-Whitney test after testing the distribution of the data. Differences between multiple groups were analyzed by one-ANOVA followed by the Student-Newman-Keuls *post hoc* test (Graphpad Prism 7.0, USA) after testing the data for equal variance. All values were expressed as mean ± SEM. Statistical significance was accepted at  $P < 0.05$ .

### **Abbreviations**

AIS, acute ischemic stroke; BCA, Bradford protein assay; CCA, common carotid artery; CCK-8, cell counting kit-8; CITED2, Cbp/p300 interacting

transactivator with Glu/Asp rich carboxy-terminal domain 2; CO<sub>2</sub>, carbon dioxide; DMEM, Dulbecco's Modified Eagle Medium; ECA, external carotid artery; ECM, endothelial cell medium; EDN1, endothelin 1; EDTA, ethylene diamine tetraacetic acid; FBS, fetal bovine serum; FITC, fluorescein isothiocyanate; HRP, horseradish peroxidase; HUVEC, Human Umbilical Vein Endothelial Cell; ICA, internal carotid artery; MCAO, middle cerebral artery occlusion; miR-191, miR-191-5p; miR-191i, miR-191 inhibitor; miR-191m, miR-191 mimic; miRNA, microRNA; MMP, matrix metalloproteinase; MRI, magnetic resonance imaging; N<sub>2</sub>, nitrogen; NCi, negative control of inhibitor; NCM, negative control of mimic; O<sub>2</sub>, oxygen; OGD/R, oxygen-glucose deprivation/reoxygenation; PBS, phosphate buffer saline; PI, propidium iodide; qRT-PCR, quantitative real-time polymerase chain reaction; RNA, ribonucleic acid; STMN1, stathmin 1; TBP, TATA-box binding protein; TTC, 2,3,5-triphenyltetrazolium chloride; UTR, Un-translated region; VEGF-A, Vascular endothelial growth factor-A; VEZF1, vascular endothelial zinc finger 1.

### **AUTHOR CONTRIBUTIONS**

Wei Gao and Xiang Lu designed the research, interpreted the data, and contributed to revising the manuscript. Kang Du and Can Zhao performed the research, analyzed the data, and wrote the manuscript. Li Wang and Yue Wang contributed to data collection and performance of rats MCAO model. Kangzhen Zhang, Xiyu Shen and Huixian Sun contributed to recruitment of patients and clinical diagnosis of disease.

### **ACKNOWLEDGMENTS**

The authors thank Ms. Weiwei Wu for her great advice and Ms. Ping Zhou for her excellent technical assistance.

### **CONFLICTS OF INTEREST**

The authors have announced no conflicts of interest.

### **FUNDING**

This work was supported by the Natural Science Foundation of China (81770440, 81700331); Postgraduate Research & Practice Innovation Program of Jiangsu Province (SJCX18\_0426); Natural Science Foundation of the Higher Education Institutions of Jiangsu Province (17KJB320003); Jiangsu Province Health Development Project with Science and Education (QNRC2016857); Natural Science Foundation of Jiangsu Province (BK20171051);The Six One Project of Jiangsu Province (LGY2018100).

## REFERENCES

1. Wei JW, Heeley EL, Wang JG, Huang Y, Wong LK, Li Z, Heritier S, Arima H, Anderson CS, and ChinaQUEST Investigators. Comparison of recovery patterns and prognostic indicators for ischemic and hemorrhagic stroke in China: the ChinaQUEST (Quality Evaluation of Stroke Care and Treatment) Registry study. *Stroke*. 2010; 41:1877–83.  
<https://doi.org/10.1161/STROKEAHA.110.586909>  
PMID:20651267
2. Powers WJ, Rabinstein AA, Ackerson T, Adeoye OM, Bambakidis NC, Becker K, Biller J, Brown M, Demaerschalk BM, Hoh B, Jauch EC, Kidwell CS, Leslie-Mazwi TM, et al, and American Heart Association Stroke Council. 2018 Guidelines for the Early Management of Patients With Acute Ischemic Stroke: A Guideline for Healthcare Professionals From the American Heart Association/American Stroke Association. *Stroke*. 2018; 49:e46–110.  
<https://doi.org/10.1161/STR.0000000000000158>  
PMID:29367334
3. Licata G, Tuttolomondo A, Corrao S, Di Raimondo D, Fernandez P, Caruso C, Avellone G, Pinto A. Immunoinflammatory activation during the acute phase of lacunar and non-lacunar ischemic stroke: association with time of onset and diabetic state. *Int J Immunopathol Pharmacol*. 2006; 19:639–46.  
<https://doi.org/10.1177/039463200601900320>  
PMID:17026849
4. Tuttolomondo A, Di Sciacca R, Di Raimondo D, Pedone C, La Placa S, Pinto A, Licata G. Effects of clinical and laboratory variables and of pretreatment with cardiovascular drugs in acute ischaemic stroke: a retrospective chart review from the GIFA study. *Int J Cardiol*. 2011; 151:318–22.  
<https://doi.org/10.1016/j.ijcard.2010.06.005>  
PMID:20598761
5. Di Raimondo D, Tuttolomondo A, Buttà C, Miceli S, Licata G, Pinto A. Effects of ACE-inhibitors and angiotensin receptor blockers on inflammation. *Curr Pharm Des*. 2012; 18:4385–413.  
<https://doi.org/10.2174/138161212802481282>  
PMID:22283779
6. Ruan L, Wang B, ZhuGe Q, Jin K. Coupling of neurogenesis and angiogenesis after ischemic stroke. *Brain Res*. 2015; 1623:166–73.  
<https://doi.org/10.1016/j.brainres.2015.02.042>  
PMID:25736182
7. Fraisl P, Mazzone M, Schmidt T, Carmeliet P. Regulation of angiogenesis by oxygen and metabolism. *Dev Cell*. 2009; 16:167–79.  
<https://doi.org/10.1016/j.devcel.2009.01.003>  
PMID:19217420
8. Phng LK, Gerhardt H. Angiogenesis: a team effort coordinated by notch. *Dev Cell*. 2009; 16:196–208.  
<https://doi.org/10.1016/j.devcel.2009.01.015>  
PMID:19217422
9. Suárez Y, Fernández-Hernando C, Yu J, Gerber SA, Harrison KD, Pober JS, Iruela-Arispe ML, Merkenschlager M, Sessa WC. Dicer-dependent endothelial microRNAs are necessary for postnatal angiogenesis. *Proc Natl Acad Sci USA*. 2008; 105:14082–87.  
<https://doi.org/10.1073/pnas.0804597105>  
PMID:18779589
10. Poliseño L, Tuccoli A, Mariani L, Evangelista M, Citti L, Woods K, Mercatanti A, Hammond S, Rainaldi G. MicroRNAs modulate the angiogenic properties of HUVECs. *Blood*. 2006; 108:3068–71.  
<https://doi.org/10.1182/blood-2006-01-012369>  
PMID:16849646
11. Suárez Y, Fernández-Hernando C, Pober JS, Sessa WC. Dicer dependent microRNAs regulate gene expression and functions in human endothelial cells. *Circ Res*. 2007; 100:1164–73.  
<https://doi.org/10.1161/01.RES.0000265065.26744.17>  
PMID:17379831
12. Bartel DP. Metazoan MicroRNAs. *Cell*. 2018; 173:20–51.  
<https://doi.org/10.1016/j.cell.2018.03.006>  
PMID:29570994
13. Tiedt S, Prestel M, Malik R, Schieferdecker N, Duering M, Kautzky V, Stoycheva I, Böck J, Northoff BH, Klein M, Dorn F, Krohn K, Teupser D, et al. RNA-Seq Identifies Circulating miR-125a-5p, miR-125b-5p, and miR-143-3p as Potential Biomarkers for Acute Ischemic Stroke. *Circ Res*. 2017; 121:970–80.  
<https://doi.org/10.1161/CIRCRESAHA.117.311572>  
PMID:28724745
14. Jeyaseelan K, Lim KY, Armugam A. MicroRNA expression in the blood and brain of rats subjected to transient focal ischemia by middle cerebral artery occlusion. *Stroke*. 2008; 39:959–66.  
<https://doi.org/10.1161/STROKEAHA.107.500736>  
PMID:18258830
15. Kulshreshtha R, Ferracin M, Wojcik SE, Garzon R, Alder H, Agosto-Perez FJ, Davuluri R, Liu CG, Croce CM, Negrini M, Calin GA, Ivan M. A microRNA signature of hypoxia. *Mol Cell Biol*. 2007; 27:1859–67.  
<https://doi.org/10.1128/MCB.01395-06>  
PMID:17194750
16. Lee HT, Chang YC, Tu YF, Huang CC. VEGF-A/VEGFR-2 signaling leading to cAMP response element-binding protein phosphorylation is a shared pathway underlying the protective effect of preconditioning on

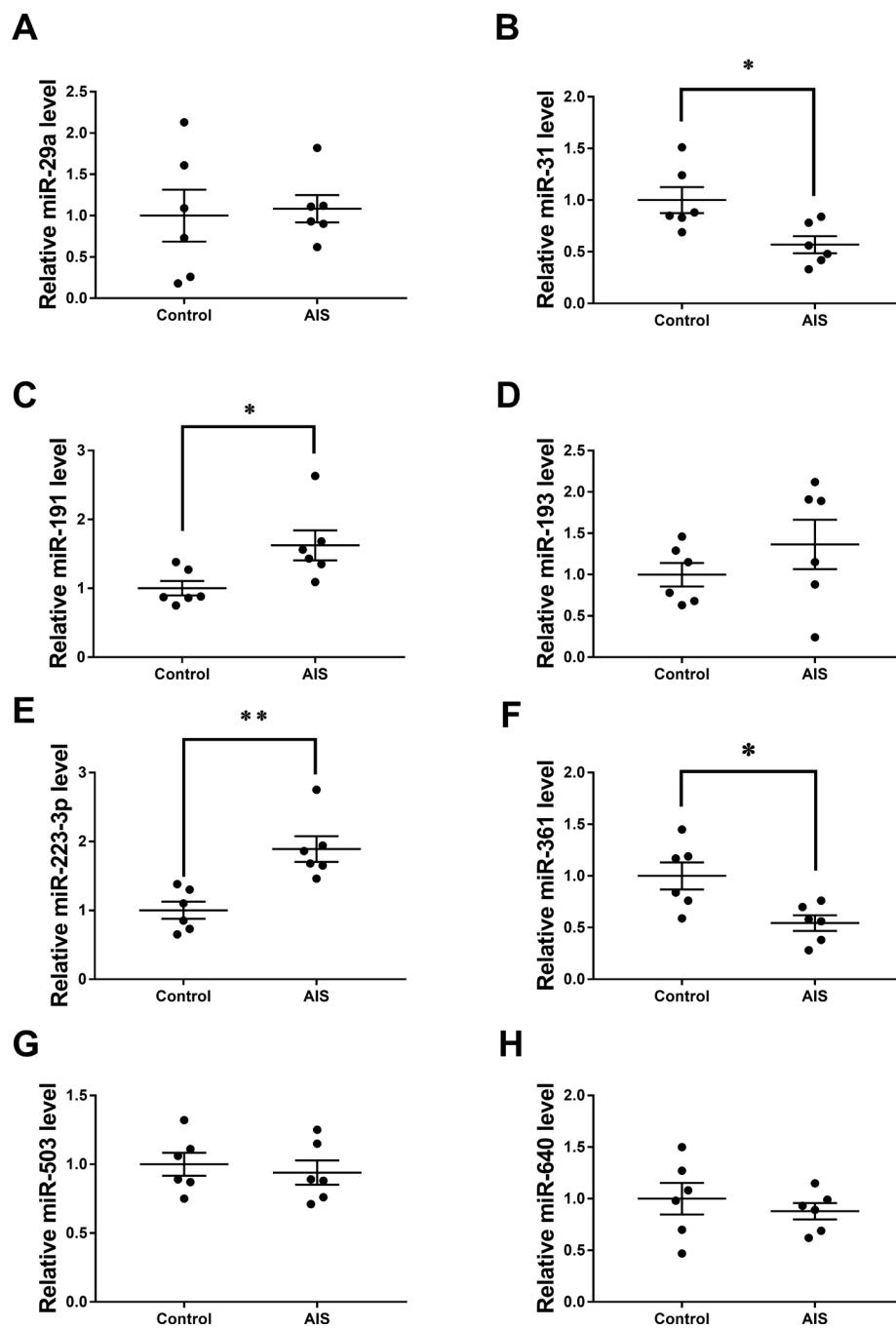
- neurons and endothelial cells. *J Neurosci.* 2009; 29:4356–68.  
<https://doi.org/10.1523/JNEUROSCI.5497-08.2009>  
 PMID:19357264
17. Wu CC, Chen YC, Chang YC, Wang LW, Lin YC, Chiang YL, Ho CJ, Huang CC. Human umbilical vein endothelial cells protect against hypoxic-ischemic damage in neonatal brain via stromal cell-derived factor 1/C-X-C chemokine receptor type 4. *Stroke.* 2013; 44:1402–09.  
<https://doi.org/10.1161/STROKEAHA.111.000719>  
 PMID:23449265
  18. Fasanaro P, D'Alessandra Y, Di Stefano V, Melchionna R, Romani S, Pompilio G, Capogrossi MC, Martelli F. MicroRNA-210 modulates endothelial cell response to hypoxia and inhibits the receptor tyrosine kinase ligand Ephrin-A3. *J Biol Chem.* 2008; 283:15878–83.  
<https://doi.org/10.1074/jbc.M800731200>  
 PMID:18417479
  19. Lou YL, Guo F, Liu F, Gao FL, Zhang PQ, Niu X, Guo SC, Yin JH, Wang Y, Deng ZF. miR-210 activates notch signaling pathway in angiogenesis induced by cerebral ischemia. *Mol Cell Biochem.* 2012; 370:45–51.  
<https://doi.org/10.1007/s11010-012-1396-6>  
 PMID:22833359
  20. Parikh VN, Jin RC, Rabello S, Gulbahce N, White K, Hale A, Cottrill KA, Shaik RS, Waxman AB, Zhang YY, Maron BA, Hartner JC, Fujiwara Y, et al. MicroRNA-21 integrates pathogenic signaling to control pulmonary hypertension: results of a network bioinformatics approach. *Circulation.* 2012; 125:1520–32.  
<https://doi.org/10.1161/CIRCULATIONAHA.111.060269> PMID:22371328
  21. Buller B, Liu X, Wang X, Zhang RL, Zhang L, Hozeska-Solgot A, Chopp M, Zhang ZG. MicroRNA-21 protects neurons from ischemic death. *FEBS J.* 2010; 277:4299–307.  
<https://doi.org/10.1111/j.1742-4658.2010.07818.x> PMID:20840605
  22. Chistiakov DA, Orekhov AN, Bobryshev YV. The role of miR-126 in embryonic angiogenesis, adult vascular homeostasis, and vascular repair and its alterations in atherosclerotic disease. *J Mol Cell Cardiol.* 2016; 97:47–55.  
<https://doi.org/10.1016/j.yjmcc.2016.05.007>  
 PMID:27180261
  23. Long G, Wang F, Li H, Yin Z, Sandip C, Lou Y, Wang Y, Chen C, Wang DW. Circulating miR-30a, miR-126 and let-7b as biomarker for ischemic stroke in humans. *BMC Neurol.* 2013; 13:178.  
<https://doi.org/10.1186/1471-2377-13-178>  
 PMID:24237608
  24. Yang D, Wang J, Xiao M, Zhou T, Shi X. Role of Mir-155 in Controlling HIF-1 $\alpha$  Level and Promoting Endothelial Cell Maturation. *Sci Rep.* 2016; 6:35316.  
<https://doi.org/10.1038/srep35316> PMID:27731397
  25. Liu DZ, Tian Y, Ander BP, Xu H, Stamova BS, Zhan X, Turner RJ, Jickling G, Sharp FR. Brain and blood microRNA expression profiling of ischemic stroke, intracerebral hemorrhage, and kainate seizures. *J Cereb Blood Flow Metab.* 2010; 30:92–101.  
<https://doi.org/10.1038/jcbfm.2009.186>  
 PMID:19724284
  26. Wang HW, Huang TS, Lo HH, Huang PH, Lin CC, Chang SJ, Liao KH, Tsai CH, Chan CH, Tsai CF, Cheng YC, Chiu YL, Tsai TN, et al. Deficiency of the microRNA-31-microRNA-720 pathway in the plasma and endothelial progenitor cells from patients with coronary artery disease. *Arterioscler Thromb Vasc Biol.* 2014; 34:857–69.  
<https://doi.org/10.1161/ATVBAHA.113.303001>  
 PMID:24558106
  27. Dai GH, Ma PZ, Song XB, Liu N, Zhang T, Wu B. MicroRNA-223-3p inhibits the angiogenesis of ischemic cardiac microvascular endothelial cells via affecting RPS6KB1/hif-1 $\alpha$  signal pathway. *PLoS One.* 2014; 9:e108468.  
<https://doi.org/10.1371/journal.pone.0108468>  
 PMID:25313822
  28. Xu W, Luo F, Sun B, Ye H, Li J, Shi L, Liu Y, Lu X, Wang B, Wang Q, Liu Q, Zhang A. HIF-2 $\alpha$ , acting *via* miR-191, is involved in angiogenesis and metastasis of arsenite-transformed HBE cells. *Toxicol Res (Camb).* 2015; 5:66–78.  
<https://doi.org/10.1039/C5TX00225G>  
 PMID:30090327
  29. Dal Monte M, Landi D, Martini D, Bagnoli P. Antiangiogenic role of miR-361 in human umbilical vein endothelial cells: functional interaction with the peptide somatostatin. *Naunyn Schmiedebergs Arch Pharmacol.* 2013; 386:15–27.  
<https://doi.org/10.1007/s00210-012-0808-1>  
 PMID:23128854
  30. Yang Z, Wu L, Zhu X, Xu J, Jin R, Li G, Wu F. MiR-29a modulates the angiogenic properties of human endothelial cells. *Biochem Biophys Res Commun.* 2013; 434:143–49.  
<https://doi.org/10.1016/j.bbrc.2013.03.054>  
 PMID:23541945
  31. Zhou Y, Li XH, Zhang CC, Wang MJ, Xue WL, Wu DD, Ma FF, Li WW, Tao BB, Zhu YC. Hydrogen sulfide promotes angiogenesis by downregulating miR-640 via the VEGFR2/mTOR pathway. *Am J Physiol Cell Physiol.* 2016; 310:C305–17.  
<https://doi.org/10.1152/ajpcell.00230.2015>  
 PMID:26879375
  32. Khoo CP, Roubelakis MG, Schrader JB, Tsaknakis G,

- Konietzny R, Kessler B, Harris AL, Watt SM. miR-193a-3p interaction with HMGB1 downregulates human endothelial cell proliferation and migration. *Sci Rep*. 2017; 7:44137. <https://doi.org/10.1038/srep44137> PMID:28276476
33. Wen Y, Chen R, Zhu C, Qiao H, Liu Y, Ji H, Miao J, Chen L, Liu X, Yang Y. MiR-503 suppresses hypoxia-induced proliferation, migration and angiogenesis of endothelial progenitor cells by targeting Apelin. *Peptides*. 2018; 105:58–65. <https://doi.org/10.1016/j.peptides.2018.05.008> PMID:29800588
34. Zhang ZG, Zhang L, Tsang W, Soltanian-Zadeh H, Morris D, Zhang R, Goussev A, Powers C, Yeich T, Chopp M. Correlation of VEGF and angiopoietin expression with disruption of blood-brain barrier and angiogenesis after focal cerebral ischemia. *J Cereb Blood Flow Metab*. 2002; 22:379–92. <https://doi.org/10.1097/00004647-200204000-00002> PMID:11919509
35. Gu Y, Ampofo E, Menger MD, Laschke MW. miR-191 suppresses angiogenesis by activation of NF-κB signaling. *FASEB J*. 2017; 31:3321–33. <https://doi.org/10.1096/fj.201601263R> PMID:28424351
36. Aitsebaomo J, Kingsley-Kallesen ML, Wu Y, Quertermous T, Patterson C. Vezf1/DB1 is an endothelial cell-specific transcription factor that regulates expression of the endothelin-1 promoter. *J Biol Chem*. 2001; 276:39197–205. <https://doi.org/10.1074/jbc.M105166200> PMID:11504723
37. Miyashita H, Kanemura M, Yamazaki T, Abe M, Sato Y. Vascular endothelial zinc finger 1 is involved in the regulation of angiogenesis: possible contribution of stathmin/OP18 as a downstream target gene. *Arterioscler Thromb Vasc Biol*. 2004; 24:878–84. <https://doi.org/10.1161/01.ATV.0000126373.52450.3> PMID:15031128
38. Miyashita H, Sato Y. Metallothionein 1 is a downstream target of vascular endothelial zinc finger 1 (VEZF1) in endothelial cells and participates in the regulation of angiogenesis. *Endothelium*. 2005; 12:163–70. <https://doi.org/10.1080/10623320500227101> PMID:16162438
39. AlAbdi L, He M, Yang Q, Norvil AB, Gowher H. The transcription factor Vezf1 represses the expression of the antiangiogenic factor Cited2 in endothelial cells. *J Biol Chem*. 2018; 293:11109–18. <https://doi.org/10.1074/jbc.RA118.002911> PMID:29794136
40. Suárez Y, Sessa WC. MicroRNAs as novel regulators of angiogenesis. *Circ Res*. 2009; 104:442–54. <https://doi.org/10.1161/CIRCRESAHA.108.191270> PMID:19246688
41. Pan W, Wang L, Zhang XF, Zhang H, Zhang J, Wang G, Xu P, Zhang Y, Hu P, Zhang XD, Du RL, Wang H. Hypoxia-induced microRNA-191 contributes to hepatic ischemia/reperfusion injury through the ZONAB/Cyclin D1 axis. *Cell Death Differ*. 2019; 26:291–305. <https://doi.org/10.1038/s41418-018-0120-9> PMID:29769640
42. Wu XQ, Tian XY, Wang ZW, Wu X, Wang JP, Yan TZ. miR-191 secreted by platelet-derived microvesicles induced apoptosis of renal tubular epithelial cells and participated in renal ischemia-reperfusion injury via inhibiting CBS. *Cell Cycle*. 2019; 18:119–29. <https://doi.org/10.1080/15384101.2018.1542900> PMID:30394829
43. Bruderer M, Alini M, Stoddart MJ. Role of HOXA9 and VEZF1 in endothelial biology. *J Vasc Res*. 2013; 50:265–78. <https://doi.org/10.1159/000353287> PMID:23921720
44. Kuhnert F, Campagnolo L, Xiong JW, Lemons D, Fitch MJ, Zou Z, Kiesses WB, Gardner H, Stuhlmann H. Dosage-dependent requirement for mouse Vezf1 in vascular system development. *Dev Biol*. 2005; 283:140–56. <https://doi.org/10.1016/j.ydbio.2005.04.003> PMID:15882861
45. Xiong JW, Leahy A, Lee HH, Stuhlmann H. Vezf1: A Zn finger transcription factor restricted to endothelial cells and their precursors. *Dev Biol*. 1999; 206:123–41. <https://doi.org/10.1006/dbio.1998.9144> PMID:9986727
46. Zou Z, Ocaya PA, Sun H, Kuhnert F, Stuhlmann H. Targeted Vezf1-null mutation impairs vascular structure formation during embryonic stem cell differentiation. *Arterioscler Thromb Vasc Biol*. 2010; 30:1378–88. <https://doi.org/10.1161/ATVBAHA.109.200428> PMID:20431070
47. Gerald D, Adini I, Shechter S, Perruzzi C, Varnau J, Hopkins B, Kazerounian S, Kurschat P, Blachon S, Khedkar S, Bagchi M, Sherris D, Prendergast GC, et al. RhoB controls coordination of adult angiogenesis and lymphangiogenesis following injury by regulating VEZF1-mediated transcription. *Nat Commun*. 2013; 4:2824. <https://doi.org/10.1038/ncomms3824> PMID:24280686
48. Longa EZ, Weinstein PR, Carlson S, Cummins R. Reversible middle cerebral artery occlusion without

craniectomy in rats. *Stroke*. 1989; 20:84–91.  
<https://doi.org/10.1161/01.STR.20.1.84>  
PMID:2643202

49. Schäbitz WR, Weber J, Takano K, Sandage BW, Locke KW, Fisher M. The effects of prolonged treatment with citicoline in temporary experimental focal ischemia. *J Neurol Sci*. 1996; 138:21–25.  
[https://doi.org/10.1016/0022-510X\(95\)00341-X](https://doi.org/10.1016/0022-510X(95)00341-X)  
PMID:8791234
50. Ferro A, Queen LR, Priest RM, Xu B, Ritter JM, Poston L, Ward JP. Activation of nitric oxide synthase by beta 2-adrenoceptors in human umbilical vein endothelium in vitro. *Br J Pharmacol*. 1999; 126:1872–80. <https://doi.org/10.1038/sj.bjp.0702512>  
PMID:10372832
51. Zhao C, Li H, Zhao XJ, Liu ZX, Zhou P, Liu Y, Feng MJ. Heat shock protein 60 affects behavioral improvement in a rat model of Parkinson's disease grafted with human umbilical cord mesenchymal stem cell-derived dopaminergic-like neurons. *Neurochem Res*. 2016; 41:1238–49.  
<https://doi.org/10.1007/s11064-015-1816-6>  
PMID:26758268

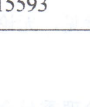
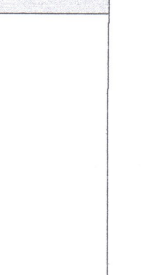

## SUPPLEMENTARY MATERIALS



**Supplementary Figure 1. Relative miRNAs levels.** Expression levels of miRNAs in Cohort A (n=6) (A) miR-29a, (B) miR-31, (C) miR-191, (D) miR-193, (E) miR-223-3p, (F) miR-361, (G) miR-503, (H) miR-640.

## 伦理审查批准件

项目伦审编号：2018-SR-25

试验项目名称	急性脑梗死患者外周血 miR-191 异常表达的作用及机制研究		
药物类别/期别	临床科研	申请专业	老年医学科
申办单位	南京医科大学附属逸夫医院	组长单位	
专业负责人	鲁翔	职务/职称	主任医师
主要研究者	鲁翔	职务/职称	主任医师
审查材料	试验方案, V1.0, 版本日期: 2018年12月10日; 知情同意书, 版本号: 02, 版本日期: 2018年12月28日; 研究者履历及参加人员列表	审查途径	<input checked="" type="checkbox"/> 会议审查 <input type="checkbox"/> 快速审查
本伦理委员会联系方式	地址: 南京市龙眠大道109号南京医科大学附属逸夫医院 电话: 025-87115593 邮箱: IRB@njmu.edu.cn		
伦理委员会列席人员签名	详见附表		
<b>伦理委员会审评意见</b>			
<p>经本伦理委员会审查, 同意进行该项临床试验。</p> <p>意见及建议: <input checked="" type="checkbox"/>无 <input type="checkbox"/>有</p> <p>该研究的进行过程中将受伦理委员会的持续审查? <input checked="" type="checkbox"/>是 <input type="checkbox"/>否</p> <p>审查频度为研究批准之日起: <input type="checkbox"/>3个月 <input type="checkbox"/>6个月 <input checked="" type="checkbox"/>1年</p> <p>伦理审查委员会有权根据实际进展情况改变持续审查频度。</p>			
<p>主任委员签名: </p> <p style="text-align: right;">   </p>			

Supplementary Figure 2. Ethical approval of Ethics Committee of Sir Run Run Hospital, Nanjing Medical University (Protocol Numbers: 2018-SR-25)

动物实验伦理审查同意书

Affidavit of Approval of Animal Ethical and Welfare

申请编号	11586	批准编号 Approval No.	IACUC-1806010
------	-------	----------------------	---------------

本《动物实验方案》经过实验动物伦理委员会审核，符合动物保护、动物福利和伦理原则，符合国家实验动物福利伦理的相关规定。方案的相关信息如下：

The animal use protocol listed below has been reviewed and approved by the Animal Ethical and Welfare Committee(AEWC).

实验名称 Protocol Title	大鼠大脑中动脉栓塞 (MCAO) 模型miRNA表达的研究 Expression of miRNAs in middle cerebral artery occlusion(MACO)				
申请人姓名 Applicant	杜康	职称/学位 Title/Degree	博士研究生	邮箱 Email	dukang@njmu.edu.cn
	Du Kang		phd. student		
实验负责人 Principle Investigator	鲁翔	职称/学位 Title/Degree	教授	邮箱 Email	luxiang66@njmu.edu.cn
	Lu Xiang		professor		
院系(部门) Department	附属逸夫医院老年医学科 Department of Geriatrics, Sir Run Run Hospital, Nanjing Medical University			申请日期 Application Date	2018-06-06
拟实验时间 Period of Protocol	2018-07-01 - 2020-06-01	实验动物使用许可证 Number of Animal Use Permit	SYXK(苏)2016-0016		
审核意见 Results of Inspection	<input checked="" type="checkbox"/> 符合动物福利伦理要求，可以进行实验。 Agree <input type="checkbox"/> 调整方案后，可以进行实验。 Agree after modify				
兽医师 Chief Veterinary Officer	张爱华 Zhangaihua		日期 Date	2018.6.15	

南京医科大学实验动物福利伦理审查委员会  
Animal Ethical and Welfare Committee of NJMU

主席(Chairman): 施爱民

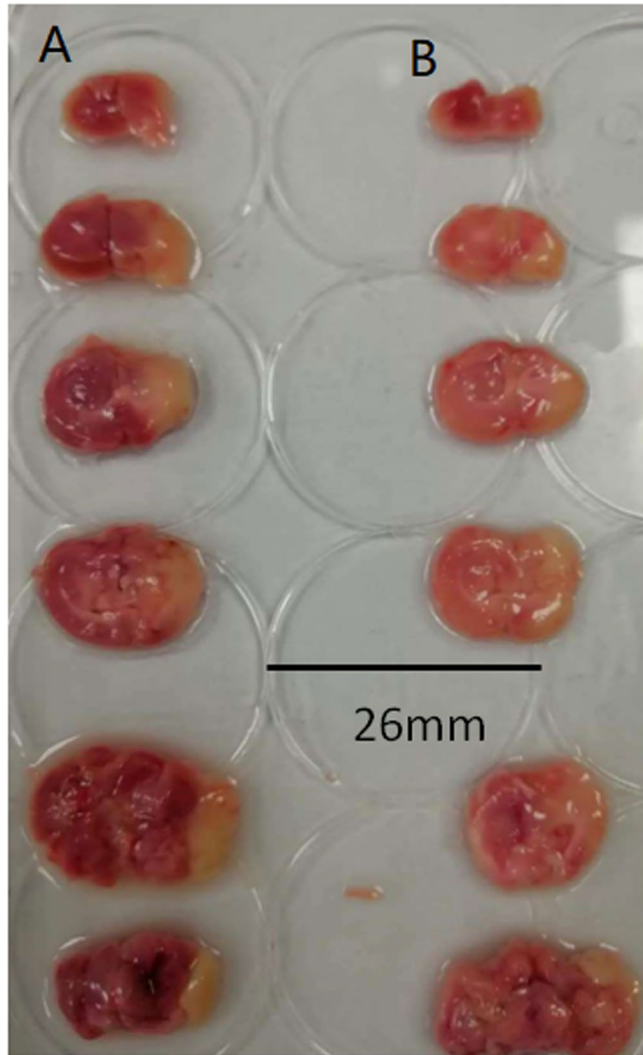
日期(Date): 2018-06-15

地址: 中国南京天元东路818号南京医科大学 邮编: 211166  
Add: Tianyun East Road 818, Nanjing Medical University, Nanjing, Jiangsu Province, P. R. China

1/11

Supplementary Figure 3. Ethical approval of Animal Ethical and Welfare Committee of Nanjing Medical University (Protocol Numbers: IACUC-1806010).





Supplementary Figure 4. TTC staining of the brains of rats MCAO.